# Department of Precision and Microsystems Engineering

**Active Vibration Control:**
**Using over-sensing and over-actuation**

Thomas van der Graaf

**TU**Delft
Delft
University of
Technology

**Challenge the future**

# Active Vibration Control
## Using over-sensing and over-actuation

by

# Thomas van der Graaf

to obtain the degree of Master of Science
at the Delft University of Technology,
to be defended publicly on Tuesday August 24, 2021 at 13:00.

Student number:     4591399
Project duration:   September 1, 2020 – August 24, 2021
Thesis committee:   S.H. HosseinNia,     TU Delft, supervisor
                    M.B. Kaczmarek,      TU Delft, daily supervisor
                    A.M. Aragón,         TU Delft
                    C. Della Santina,    TU Delft

An electronic version of this thesis is available at
http://repository.tudelft.nl/.

# CONTENTS

# PREFACE

This chapter serves as a guide for the reader on how to efficiently go through the contents of this thesis.

Chapter 1 is the introduction to the topic. The motivation for this research is explained in this chapter. First, it is explained why (active) damping is needed. Then, it is argued why over-actuation and over-sensing are expected to improve the damping performance. Finally, the gap in literature and the goals of this research are defined.

In chapter 2, a review on important topics regarding active vibration control is presented. First, some important knowledge on active vibration control (AVC) is explained in section 2.1. Secondly, the working principle of piezoelectric transducers and their use in AVC is presented in section 2.2. Then, optimization criteria on the placement of piezoelectric transducers in AVC setups are discussed and explained in section 2.3. Finally, the findings from section 2.3 are verified by an numerical model. This numerical model is discussed in detail in section 2.4, and the results are discussed.

Chapter 3 contains the main work of this thesis. This chapter is presented in a journal paper format. It should provide the reader with all the necessary information to understand the main work of this thesis. The paper starts with an introduction, followed by relevant state-of-the-art literature of important topics. Then, the method section explains the experimental setup. In this setup, over-actuation and over-sensing is implemented for active vibration control on a flexible structure. In the results section, the improvement of the over-actuation and over-sensing method compared to the state-of-the-art damping methods is shown. Finally, some conclusions are given in the paper. So, if the reader is short in time and quickly wants to know what this thesis is about, I would recommend to start reading chapter 3.

In chapter 4, the study is concluded and some interesting directions for future research are given.

The appendices in this report are mainly interesting for readers who want to recreate the work, or use some parts of the experimental setup. Appendix A explains the experimental setup and all of its components in detail. In appendix B, a step-by-step guide on how to use the LabVIEW program is presented. Appendix C shows the system identification that was performed. Finally, some practical tips for building the experimental setup are presented in appendix D.

*Thomas van der Graaf*
*Delft, August 2021*

# ACKNOWLEDGEMENTS

This thesis was performed at the Department of Precision and Microsystems Engineering, TU Delft.

I am very happy that Marcin was my daily supervisor. The weekly meetings on friday were always very interesting, and the feedback and critical thinking of Marcin has helped me to improve my work. Next to this, it was also a pleasure to discuss non study-related topics from time to time.

In addition to this, I was lucky to have Hassan as my main supervisor. The monthly meetings helped me to deepen my knowledge on active damping, and it really motivated me to work hard in order to show some progress in each meeting. Also, I appreciated the weekly monday morning meetings with all of the students under the supervision of Hassan. For me, it was a pleasure to keep in touch with some of my peer students, and to get a quick overview of what everyone was doing. This helped me to broaden my knowledge in Mechatronic System Design.

I am grateful that I got the opportunity to work in the Mechatronics lab at the 3mE faculty, especially in these uncertain covid-times. It was a pleasure to work in the lab, especially as I was often surrounded by my peer students Hani, Mathew, Romano and Roelof. For me, it really felt like we could help out each other when we got stuck in some parts. By troubleshooting together, we were able to quickly solve most of the problems. More importantly, the coffee breaks and discussions together made working in the lab a real pleasure.

Finally, I want to thank the members from Lab Support for providing me the space to work in the lab, and for making sure that I got all the hardware that I needed for my experimental setup.

*Thomas van der Graaf*
*Delft, August 2021*

# 1

# INTRODUCTION

## 1.1. MOTIVATION

Mechanical vibrations are one of the most significant sources of error in different kinds of mechanical systems. For example, vibrations in vehicles such as cars and airplanes can cause noise and discomfort for the passengers. In structural mechanics, it can cause failure of the structure, for example resonance in bridges. The field that is especially interesting is the high-tech industry, where small undesired vibrations are limiting the performance of the system. An example of such a system is a wafer stepper. In a wafer stepper, vibrations with amplitudes in the nanometer range can result in a misalignment of the wafer which will result in a failure of the production process. So, even vibrations in the nanometer range can be limiting the performance of these machines in the high-tech industry.

The high-tech industry is driven by Moore's law, which states that the number of transistors in integrated circuits doubles approximately every 24 months [1]. To facilitate further developments, the bandwidth of machines in the high-tech industry is pushed as high as possible.

In recent years, the design of machines in the high-tech precision industry has changed. Traditional joints and mechanisms are replaced by compliant mechanisms and/or flexures. These compliant mechanisms have several advantages [2]. The first major advantage is that compliant mechanisms have excellent repeatability because there is no friction, no hysteresis and no backlash. The second advantage of compliant mechanisms is that it is generally more cost effective to manufacture because there are less parts compared to traditional joints. For example, compliant mechanisms could be manufactured by additive manufacturing or laser-cutting techniques. A third benefit of compliant mechanisms is that the required maintenance is much lower compared to traditional joints. This is because the flexible mechanisms consist of a low number of parts, no lubrication is needed, there is no friction wear and also particle contamination is not as problematic compared to traditional joints. Furthermore, compliant mechanisms are perfectly suited for use in vacuum environments and they are also suited to be used at microscale.

All of the mentioned advantages are the reason why, in the recent years, compliant mechanisms are becoming more and more present in high-precision machines. However,

the introduction of compliant mechanisms into high-precision machines is problematic for the damping design of these systems. Systems are becoming more and more lightweight while the stiffness is becoming higher. In consequence, the structural damping of the system decreases. The decrease of the structural damping will result in undesired vibrations that can be caused by resonance modes of the system. Also, the compliant mechanisms often contain long flexures which have the inherent problem of multiple vibration modes. In order to keep the oscillations to a minimum, the mechanical vibrations should be damped by a damping system.

Damping is defined as dissipating vibrational energy from a mechanical system and thereby lower the resonance peaks in the frequency response function. Different methods exist for damping mechanical vibrations. In figure 1.1, three different existing damping methods are shown.



(a)                                              (b)                                              (c)
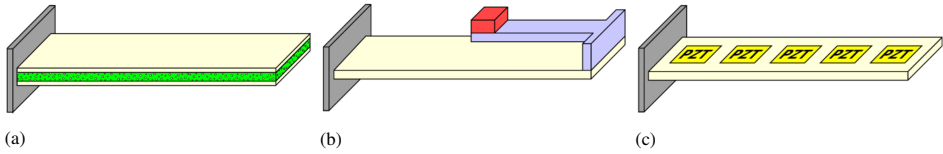
Figure 1.1: Schematic overview of different damping methods (a) Constrained Layer Damping; (b) Tuned Mass Damper; (c) Active Damping

In figure 1.1a, a schematic view of constrained layer damping (CLD) is shown. In CLD, a viscoelastic material is sandwiched between two sheets of stiff material. The viscoelastic layer will convert the kinetic energy from the vibrations into thermal energy (heat). In this way, it acts as a vibration damper.

Another possible damping method is tuned mass damper (TMD). A schematic overview of TMD can be seen in figure 1.1b. A TMD system consists of a mass that is mounted on a spring. The oscillation frequency of the mass is tuned to match te resonance frequency of the host structure. In this way, TMD can reduce the maximum vibration amplitude of the host structure. Both CLD and TMD can be classified as 'passive damping'. Passive damping systems need no external energy source and there are no sensors present. The energy is dissipated inside the system and the amount of damping is proportional to the weight. For high-tech applications where multiple vibration modes need to be suppressed, passive damping systems are generally not implemented because a passive damping system is only effective in a narrow frequency range. So, for multiple resonance modes, multiple passive damper layers (or TMD's) must be implemented. Therefore, in high-tech applications were multiple modes need to be controlled, passive damping is not the optimal solution.

The other possible method is active damping. A schematic view of an active damping system is shown in figure 1.1c. Active damping systems need sensors, control and an external energy source. The energy is dissipated outside the system and the damping can be turned on and off, which is not possible in passive damping systems. Active damping or active vibration control (AVC) is a very promising option to be implemented in high-tech systems where multiple vibration modes need to be suppressed and the system needs to have a high bandwidth. Compared to passive damping, AVC has higher damping performance, lower cost and less mass constraints. Often, piezoelectric transducers are used as both

sensors and actuators in AVC [3] [4]. The main benefits of these piezoelectric transducers are: ease of integration, low cost, vacuum-proof and usable in a wide-frequency operation range.

## 1.2. DISTRIBUTION OF SENSORS AND ACTUATORS IN ACTIVE VIBRATION CONTROL

In 1985, one of the first studies on vibration control with an active piezoelectric element was performed [5]. This study showed promising results in terms of damping performance and could be seen as the start of a new field of research: the field of 'smart structures' where sensors and actuators are used to actively control vibrations. In the following years, a lot of research has been performed on active vibration control of flexible systems. Most of these studies were focused on suppressing vibrations in flexible systems such as cantilevered beams or plates. Figure 2 shows the general setup that is often used for the vibration control of a flexible beam. In this figure, collocated sensors and actuators can be seen. The collocation of sensors and actuators will be described in more detail in section 2.1.1. The information about the deformation of the beam is obtained from the sensors. This data is then provided to a control algorithm, which will output a control voltage that will be applied to the piezoelectric actuators. This continuous loop is referred to as the active vibration control system.
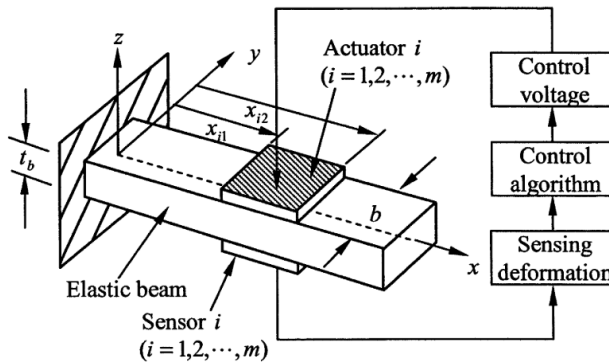


Figure 1.2: General AVC setup: beam model with collocated sensors and actuators [6]

In the present scientific literature, many examples can be found where an attempt is made to suppress the vibrations in a flexible beam by using a so called 'smart' beam that contains piezoelectric sensors and actuators. From a recent literature review on active vibration control in flexible beams by [7], it can be concluded that all of the present studies have a number of sensor/actuator pairs that is lower than or equal to the desired number of modes to be controlled. These two methods will be described in the next subsections, and examples of studies where these methods are employed are discussed.

### 1.2.1. UNDER-ACTUATION AND UNDER-SENSING

In under-actuation, the number of actuators is lower than the number of controlled modes. Similarly, in under-sensing, the number of sensors is lower than the number of controlled modes. In an under-actuated system, the control algorithm is designed in such a way that one actuator is used to control multiple modes.

In literature, numerous examples of under-actuation and under-sensing in AVC are mentioned. For example, in a study performed by Bruant & Poselier, 1 sensor and 2 actuators were used to control the first 3 modes [8]. Other examples of under-actuated designs are the works of Daraji et al [9] and Zoric et al [10]. In the study performed by Daraji et al, four actuator-sensor pairs for controlling 6 modes and the setup of the study performed by Zoric et al utilizes 4 actuator-sensor pairs for the first 5 modes. In all of these three studies, vibrations could effectively be damped to a certain extent.

### 1.2.2. PERFECT-ACTUATION AND PERFECT-SENSING

In perfect-actuation and perfect-sensing, the number of actuators and sensors is equal to the number of modes to be controlled. In this way, each actuator-sensor pair is used to target one specific mode. This means that the actuators and sensors could be placed at an optimal location for the intended mode.

Similarly to under-actuation and under-sensing, numerous studies can be found in literature where perfect-actuation and perfect-sensing is used. One example of such a study is the work of Kumar et al [11], where 5 collocated sensor-actuator pairs were used to control the first 5 vibration modes. This is schematically shown in figure 1.3.
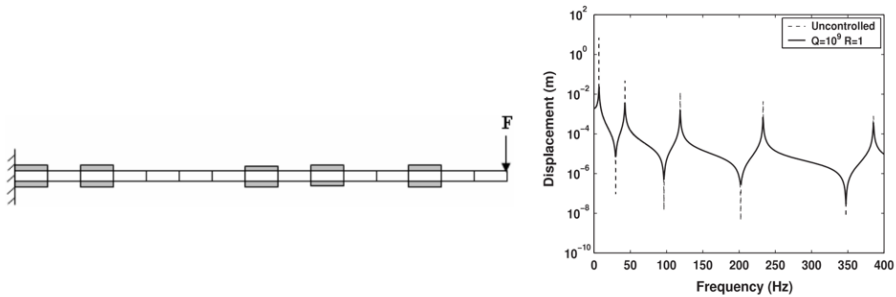
Figure 1.3: Example of perfect-actuation & perfect-sensing study [11]

Another example of a study where perfect-actuation and perfect-sensing is implemented is the work of Lu et al, where 2 actuators are used for controlling 2 modes [12].

### 1.2.3. OVER-ACTUATION IN ACTIVE VIBRATION CONTROL

Besides the well known and often used methods of under-actuation and pefect-actuation, there is another possible method called over-actuation. In over-actuation, the number of actuators is higher that the number of controlled modes.

The concept of using additional actuators has been researched extensively in motion systems for disturbance rejection. Steinbuch et al [13] proved that using additional actuators in motion control improves the modal controllability in the feedback path. The over-actuated

design allows for additional actuators exclusively for controlling the resonances excited by the external disturbances while the other actuators are placed to get the desired motion.

Another study where over-acutation is considered is [14]. Here, eigenmodes of the structure are grouped. Then, a modal force is applied on the grouped modes. The control force is applied individually on each cluster of the control system. This strategy obtained a more energy efficient method for velocity control.

Another benefit of using an over-actuation and over-sensing strategy is robustness against failures. If one actuator or sensor fails, the performance will decrease but the system will still be damped by the other sensor-actuator pairs.

Next to beam-like structures, active vibration control is also often applied in plate-like structures, where both bending and torsional vibration modes are present. In the literature review [15], it has been shown that the suppression of plate-like structures with piezoelectric transducers is a field of research that has been researched extensively in the past few years. In this review, a list of vibration controller architectures with host structure types is presented. All of the studies that are reviewed by [15] are either in the under-actuation & under-sensing configuration or in the perfect-actuation & perfect-sensing configuration.

## 1.3. RESEARCH GAP

As explained this chapter (and also in chapter 2), a lot of research has been performed on active vibration control. Different controllers have been researched and tested. Also, several studies have been performed on the optimal placement of piezoelectric sensors and actuators in AVC (see section 2.3). However, to the best of the writers knowledge, in all of the work present in state-of-the art literature distributed over-actuation and over-sensing has not been studied.

The recent work done by [16] was the first study that included distributed over-actuation in an AVC system. In this work, it was showed that an AVC system that uses distributed over-actuation has significant benefits in terms of damping performance compared to 'traditional' AVC systems, where the number of actuators is less than or equal to the number of modes to be controlled. While the over-actuated setup showed significant improvements in the damping performance, the literature suggests that combining over-actuation with over-sensing could result in an even better damping performance. More details on this work will be explained in section 2.5.

If over-actuation and over-sensing would be combined, a fully collocated setup is created. As will be explained in more detail in section 2.1, collocated control systems are robustly stable. Also, it is possible to create a decentralized control structure by using only collocated sensor-actuator pairs. All in all, the gap in the current research on the distribution of sensors and actuators in AVC is that there are no studies were both over-sensing and over-actuation are used. This gap will be addressed in this thesis project.

## 1.4. RESEARCH OBJECTIVES

As explained in section 1.3, there are no studies where both over-actuation and over-sensing are used in AVC. The goal of this work is to adress this research gap. The most important question that will be answered in this research is:

**1**

*How could over-actuation and over-sensing improve the damping performance in active vibration control systems?*

The following sub-questions are relevant for this general main research question.

- *What is the optimal placement for the sensors and actuators in an active vibration control system?*

- *How can over-actuation and over-sensing be implemented in a physical active vibration control system?*

- *How does the damping performance of the over-sensed and over-actuated setup compare to other active vibration control setups?*

From these questions, the following research objectives are defined:

- Design a setup with a distribution of sensors and actuators such that an over-actuated and over-sensed setup is created. The sensors and actuators should placed at the optimal locations, and the design should be created in a structured way.

- Create this design in a real-life experimental test setup in the lab

- Validate the working of the new strategy in an experimental test setup and compare the damping performance to existing strategies.

To validate the hypothesis that a combination of over-sensing and over-actuation will result in a better damping performance, a comparative (experimental) study will be performed where the following configurations will be tested and compared:

1. Perfect-sensing & perfect-actuation

2. Perfect-sensing & over-actuation

3. Over-sensing & over-actuation

From this list, the first configuration is a configuration that is commonly used in recent studies [7]. The second configuration is one that is studied for the first time in a recent study by [16]. This already showed an improvement in damping performance. The third setup has not been studied before. It is expected that the setup with over-sensing and over-actuation has an even better damping performance, for the reasons mentioned in this chapter. The goal of this research is to implement AVC on a flexible beam, using an over-sensing and over-actuation approach. In an experimental way, the damping performance will be compared with previously studied method.

## REFERENCES

[1]  Moore, G. E. (1965). Cramming more components onto integrated circuits.

[2]  Larry L Howell, Spencer P Magleby, Brian Mark Olsen, and John Wiley. *Handbook of compliant mechanisms*. Wiley Online Library, 2013.

[3] A. Preumont. *Vibration Control of Active Structures: An Introduction.* Solid Mechanics and Its Applications. Springer, 2013. ISBN 9789400720336.

[4] SO Reza Moheimani and Andrew J Fleming. *Piezoelectric transducers for vibration control and damping.* Springer Science & Business Media, 2006.

[5] Thomas Bailey and James E Hubbard Jr. Distributed piezoelectric-polymer active vibration control of a cantilever beam. *Journal of Guidance, Control, and Dynamics,* 8(5):605–611, 1985.

[6] Yaowen Yang, Zhanli Jin, and Chee Kiong Soh. Integrated optimal design of vibration control system for smart beams using genetic algorithms. *Journal of Sound and Vibration,* 282(3-5):1293–1307, 2005.

[7] P. Shivashankar and S. Gopalakrishnan. Review on the use of piezoelectric materials for active vibration, noise, and flow control. *Smart Materials and Structures,* 29(5):053001, 2020.

[8] Bruant, I., & Proslier, L. (2015). Improved active control of a functionally graded material beam with piezoelectric patches. *Journal of Vibration and Control*, 21(10), 2059-2080.

[9] Daraji, A. H., Hale, J. M., & Ye, J. (2018). New methodology for optimal placement of piezoelectric sensor/actuator pairs for active vibration control of flexible structures. *Journal of Vibration and Acoustics*, 140(1).

[10] Zorić, N. D., Simonović, A. M., Mitrović, Z. S., & Stupar, S. N. (2013). Optimal vibration control of smart composite beams with optimal size and location of piezoelectric sensing and actuation. *Journal of Intelligent Material Systems and Structures*, 24(4), 499-526.

[11] K Ramesh Kumar and S Narayanan. Active vibration control of beams with optimal placement of piezoelectric sensor/actuator pairs. *Smart Materials and Structures,* 17 (5):055008, 2008.

[12] Lu, E., Li, W., Yang, X., Wang, Y., & Liu, Y. (2018). Optimal placement and active vibration control for piezoelectric smart flexible manipulators using modal $H_2$ norm. *Journal of Intelligent Material Systems and Structures*, 29(11), 2333-2343.

[13] M. Schneiders MJG van de Molengraft and M. Steinbuch, "*Benefits of overactuation in motion systems,*" tech. rep., 2004.

[14] N. Tanaka and S. D. Snyder, "Cluster control of a distributed-parameter planar structure—Middle authority control," *The Journal of the Acoustical Society of America,* vol. 112, pp. 2798–2807, 12 2002.

[15] Ugur Aridogan and Ipek Basdogan. A review of active vibration and noise suppression of plate-like structures with piezoelectric transducers. *Journal of Intelligent Material Systems and Structures,* 26(12):1455–1476, 2015.

[16] Madhan Gopal Muruganandam Mallur. A comparative study on distributed active damping of flexible systems. *Master Thesis TU Delft*, 2020.

# 2

# LITERATURE REVIEW

## 2.1. ACTIVE VIBRATION CONTROL

In active damping, the primary objective of the controller is to increase the negative real part of the system poles, while maintaining the natural frequencies essentialy unchanged [1]. This will attenuate the magnitude of the resonance peak in the dynamic amplification. In general, the goal of a certain active damping system is to reduce the magnitude of the resonance peaks in the frequency response function. The role of damping in a system is shown in figure 3.2, where both the pole locations and the dynamic amplification plots can be seen.
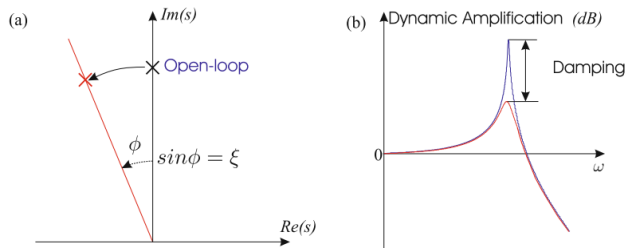


Figure 2.1: Role of Damping [1] (a) System poles, (b) Dynamic amplification

In this section, several topics regarding the control system are discussed. First, collocated systems and its benefits will be explained, then centralized and decentralized control will be explained and compared and finally some control strategies that are commonly used in state-of-the-art research will be explained.

### 2.1.1. COLLOCATED SYSTEM

A collocated control system is a system where the sensor and actuator are attached to the same degree of freedom and the sensor and actuator are dual. A dual sensor and actuator is for example a force actuator and displacement sensor, or a torque actuator and rotational

sensor. In dual systems, the product of the sensor signal and the actuator signal represents the energy exchange between the host structure and the control system. The open-loop FRF of a collocated control system that is assumed to be undamped is:

$$G_{kk}(\omega) = \sum_{i=1}^{m} \frac{\phi_i^2(k)}{\mu_i(\omega_i^2 - \omega^2)} + R_{kk} \qquad (2.1)$$

All the residues are positive (square of modal amplitude). As a result, $G_{kk}(\omega)$ is a monotonously increasing function of the frequency. This can be seen in figure 2.2. The magnitude of the FRF ranges from $-\infty$ at one of the resonance frequencies to $+\infty$ at the next resonance frequency. In every interval between to consequetive resonance frequencies, there is a certain frequency where the magnitude of the FRF equals zero. This is also known as 'anti-resonance' and they correspond to the purely imaginary zeros in the open-loop transfer function.
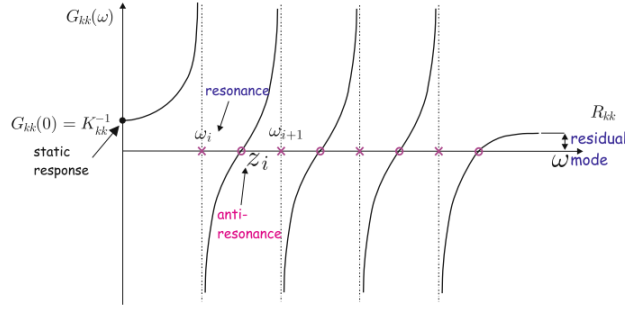


Figure 2.2: Open-loop FRF of undamped collocated system [1]

Undamped collocated control systems are systems with alternating poles and zeros, that are purely imaginary. This is shown in figure 2.3a. If the system is lightly damped, these poles and zeros get a small negative real value and therefore shift to the left-half plane. However, the poles and zeros are still in the same order, there is always a pole/zero pair.
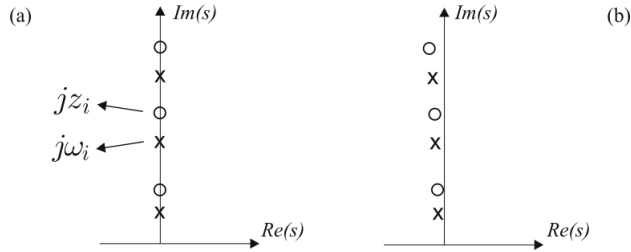


Figure 2.3: Pole/zero pattern of collocated system (a) undamped; (b) ligthly damped [1]

For non-collocated systems (systems where sensors and actuators are not attached to the same DoF), the poles and zeros are no longer present in pairs. This situation is called

pole-zero flipping and is visually shown in figure 2.4. Pole-zero flipping causes a phase uncertainty of $360^o$ which means that the system is not robustly stable.
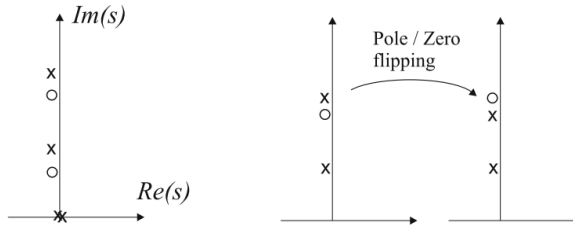


Figure 2.4: (a)Pole/zero pattern of collocated system; (b) Pole-zero flipping in non-collocated system [1]

## 2.1.2. DECENTRALIZED VS. CENTRALIZED CONTROL

For active vibration control of a flexible beam, two general strategies can be used. These strategies are centralized and decentralized control.

### CENTRALIZED CONTROL

In centralized control, data from different sensors (which are distributed along the beam) is combined and one output is computed. The result of this data combination could for example be the mode shapes and vibration amplitude.

To combine data from different sensors to compute modal information, a well known and often used technique is the modal filter. The working principle of modal filters depends on the principle of orthogonality of mode shapes. Modal filters are possible in two different configurations: continuous modal filter and discrete modal filters. In continuous modal filters, the electrode profile is shaped according to the strain distribution. Therefore, the sensor is able to only sense the mode corresponding to this electrode profile shape, because all of the other modes are orthogonal to this specific mode. However, to use a continuous modal filter for multiple modes is not practical. Different piezoelectric elements with shaped electrodes would need to be stacked on top of each other. In a discrete modal filter however, a discrete array of sensor elements are used and by the use of weighting coefficients the modal filter is created. In a (discrete) modal filter, data from the sensor array is combined using a linear combiner with certain weighting factors. If the weighting coeffecients are well chosen, the modal filter should only be sensitive to one specific mode, while the other modes are not observable. A schematic overview of the discrete modal filter is shown in figure 3.4a.

In order to use the discrete modal filter, it is required to accurately know the mode shapes in order to choose the appropriate weighting coefficient for the linear combiner [2]. As an example, the weighting coefficients for the first 4 modes of a rectangular plate are shown in figure 3.4b.

When the data of the different sensors is combined into one global measurement, a central control device will calculate the required control forces and the appropriate signals will be sent to the actuators to control the vibrations in the host structure. In such a central-
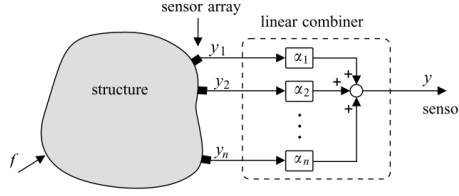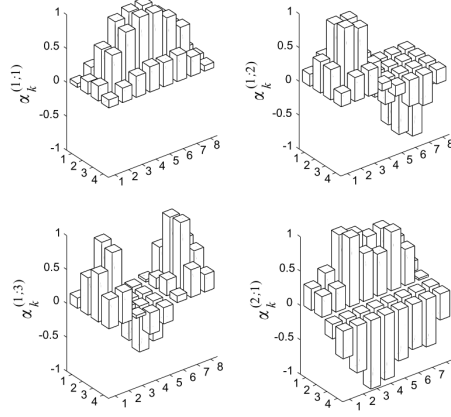
Figure 2.5: Discrete modal filter [2]



Figure 2.6: Weigthing coefficients of modal filter for the first 4 modes of a rectangular plate [2]

ized system, the requirements on data transmission and communication increase with the number of sensors and actuators used. In complex systems where the number of sensors and actuators is relatively high, these communication requirements could impose economic and technical challenges for the implementation of the feedback control system. When the dimensionality of the system increases, its required control computation will increase exponentially. [3]. Another downside of centralized control is that, in case of failure of the central controller unit, the complete control sytem is out of operation.

DECENTRALIZED CONTROL

In decentralized control however, the control problem is divided into a set of smaller subsystems. The data of different sensors is not combined and the system will consist of a number of collocated actuator/sensor pairs that each form an individual control loop. This is shown schematically in figure 2.7.

In a decentralized system, all of the computations for the individual control loops can be performed in parallel. This will add to the reliability of the system significantly [4], because only part of the feedback system will stop working when there is an operational failure in one of the controllers.

When the decentralized and centralized control methods are compared, decentralized control has the following advantages [4] [5]:
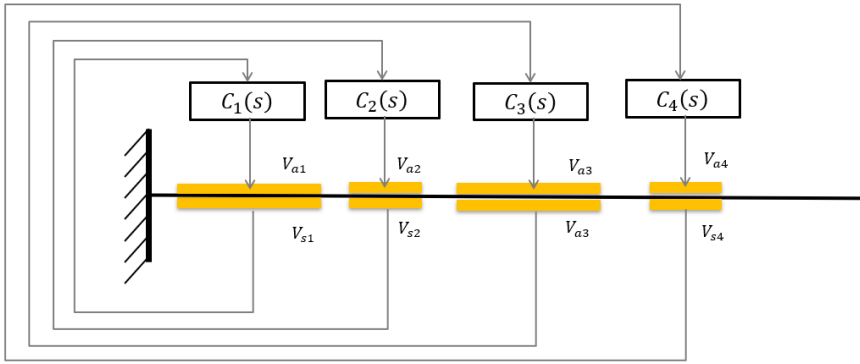
Figure 2.7: Schematic representation of decentralized control system with 4 collocated actuators/sensors

- Increased robustness and reliability against power and operational failures

- Guaranteed collocation of sensors and acutators

- Reduced complexity

- Reduced communication

- Computational efficiency; Distributed computing in real time

- Reduced energy requirements

### 2.1.3. CONTROL ALGORITHMS

Positive position feedback (PPF), direct velocity feedback (DVF) and integral resonance control (IRC) are common control algorithms that could be used to control flexible systems by using piezoelectric transducers. In this section, the different algorithms will be explained and compared.

#### INTEGRAL RESONANCE CONTROL

Integral Resonance Control (IRC) is a simple and robut control method. This algorithm is very popular in stages where piezoelectric transducers are used. In general, a displacement actuator is used in combination with a force sensor. IRC uses an integrator to add damping to the system. The block diagram of the IRC algorithm is shown in figure 2.8.

There are different options for the feedback controller in IRC. Often used options are a simple integrator ($C(s) = \frac{K}{s}$), a low-pass filter ($C(s) = \frac{K}{s+p_1}$) and a band-pass filter ($C(s) = \frac{Ks}{(s+p_1)(s+p_2)}$)
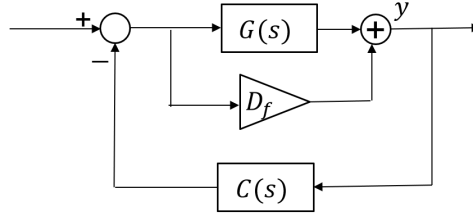
Figure 2.8: Block Diagram of IRC algorithm

## DIRECT VELOCITY FEEDBACK

In direct velocity feedback, the output signal from velocity sensors are multiplied by its gain which is then fed back to the actuators.

The DVF equation for a single DOF is:

$$\ddot{x} + 2\zeta\omega\dot{x} + \omega^2 x = \omega^2 f\dot{x} \tag{2.2}$$

where

$$f = g = \text{modal control force}$$
$$g = \text{feedback gain}$$
$$\zeta = \text{modal damping of the structure}$$
$$\omega = \text{natural frequency of the structure}$$
$$x = \text{modal coordinate of the structure}$$

Equation 2.2 can be rewritten into equation 2.3.

$$\ddot{x} + (2\zeta\omega + g\omega^2)\dot{x} + \omega^2 x = 0 \tag{2.3}$$

The damping is achieved by the gain feedback of the velocity signal that is obtained by the velocity sensor. Schematically, this is shown in figure 2.9.
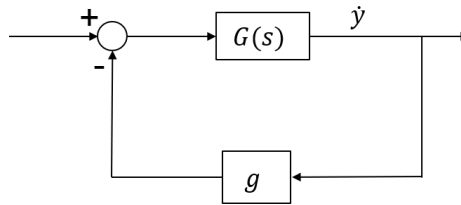


Figure 2.9: Block Diagram of DVF algorithm

Although DVF is a robustly stable control method, it has some limitations. While other control algrotihms only use much control effort near the resonance frequencies, DVF requires high control effort at all frequencies [1]. This might result in actuator saturation and therefore reduced efficiency. Also, when DVF is used with piezoelectric sensors that sense

strain, an additional differentiator is needed to differentiate the position signal into the velocity signal that is needed. Because of these limitations, DVF is generally not preferred as a control algorithm in an AVC system with piezoelectric sensors and actuators.

### POSITIVE POSTION FEEDBACK

Positive Position Feedback (PPF) is a popular control method for collocated systems. This method has been introduced by Goh and Caughey. PPF introduces a second-order filter. The input of this filter is the sensed position of the host structure. The position response is positively fed back to give the force input to the system. For stability, the number of zeros should not be higher than the number of poles of the system. This is ensured by the PPF method. The second-order PPF is a filter with the following transfer function:

$$H(s) = \frac{-g}{s^2 + 2\zeta_f \omega_f s + \omega_f^2} \tag{2.4}$$

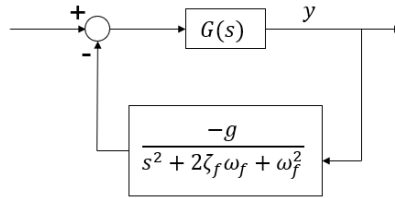The block diagram of the PPF algorithm is shown in figure 2.10.



Figure 2.10: Block Diagram of PPF algorithm

In modal domain, the equation for a single DOF system is:

$$\ddot{\xi} + 2\zeta_f \omega_f \dot{\xi} + \omega_f^2 \xi = \omega^2 f \tag{2.5}$$

The equation for the PPF compensator is:

$$\ddot{\eta} + 2\zeta_f \omega_f \dot{\eta} + \omega_f^2 \eta = \omega_f^2 \xi \tag{2.6}$$

where

$$f = g\eta = \text{modal force for the PPF}$$
$$\xi = \text{modal coordinates}$$
$$\eta = \text{Filter coordinates}$$
$$\omega \& \omega_f = \text{system and filter frequencies}$$
$$\zeta \& \zeta_f = \text{system and filter damping ratios}$$

### Tuning of PPF

The controller has three variables, $g$ (gain), $\omega_f$ (cut-off frequency) and $\zeta_f$ (damping ratio). For the most effective action, the cut-off frequency should be tuned equal to the resonance frequency of the vibration mode that needs to be damped. The two remaining variables, gain and damping ratio, can be used to tune the controller to reach the desired effect.

### Parallel PPF

To control multiple modes, PPF can be used in a parallel configuration, where each block is tuned to one specific mode. This is shown in figure 2.11.
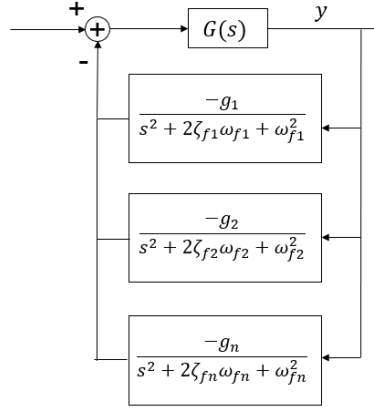


Figure 2.11: Block Diagram of parallel PPF

## 2.2. Piezoelectric Transducers in Active Vibration Control

Piezoelectric transducers are a type of actuators that are commonly used in AVC systems [1] [6]. Next to the actuation mode of these transducers, they can also be applied in sensing mode [1] [7]. The advantages of piezoelectric actuators and sensors compared to other types of actuators and sensors are [8]:

- High power density

- Fast reponse

- Large force

- High sensitivity

- Linear response

Another benefit is that piezoelectric strain sensors have a higher signal to noise ratio then conventional wire strain gages [7].

To find out how piezoelectric transducers can optimally be used in AVC, it is important to first understand the working principles. Therefore the piezoelectric phenomenon will first be explained to form a theoretical framework. Then, the application of piezoelectricity and the possible actuator and sensor configurations will be explained.

### 2.2.1. Piezoelectric phenomenon

Piezoelectric materials are a special class of materials. When mechanical stress is applied to a piezoelectric material, electric charges are produced. This is called the direct piezoelectric effect this can be used as a sensing mode. Besides the direct piezoelectric effect, it is also possible to provide electric charges to a piezoelectric material which will create mechanical deformations. This is called the converse piezoelectric effect and can be used as a actuation mode. A schematic overview of the different modes is presented in figure 2.12.
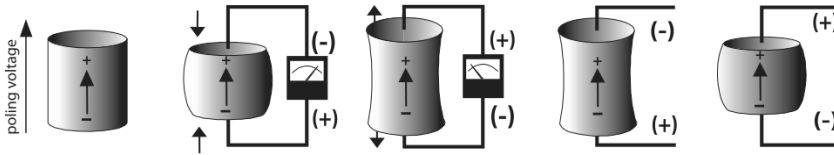


Figure 2.12: Reaction of a poled piezoelectric element to applied stimuli [9]

The constitutive equations for piezoelectric materials are: Equation 2.7 describes the situation where the piezoelectric transducer is used as an actuator and equation 2.8 describes the situation where the piezoelectric transducer is used as a sensor.

$$S_{ij} = s_{ijkl}^E T_{kl} + d_{kij} E_k \tag{2.7}$$

$$D_i = d_{ikl} T_l l + \epsilon_{ik}^T E_k \tag{2.8}$$

where

$$T_{ij} = \text{components of the stress tensor}$$
$$S_{kl} = \text{components of the strain tensor}$$
$$s_{ijkl}^E = \text{Compliance tensor under constant electric field}$$
$$E_k = \text{applied electric field}$$
$$D_i = \text{vector of electric displacements}$$
$$\epsilon_{ik}^T = \text{dielectric constant under constant stress}$$

In literature, the stress and strain tensor notations are often replaced by engineering vector notations for brevity.

**2**

$$
T = \begin{Bmatrix} T_{11} \\ T_{22} \\ T_{33} \\ T_{23} \\ T_{31} \\ T_{12} \end{Bmatrix}
\qquad\qquad
S = \begin{Bmatrix} S_{11} \\ S_{22} \\ S_{33} \\ 2S_{23} \\ 2S_{31} \\ 2S_{12} \end{Bmatrix}
\tag{2.9}
$$

With these notations, equations 2.7 and 2.8 can be written as:

$$
\{S\} = [s]\{T\} + [d]\{E\}
\tag{2.10}
$$

$$
\{D\} = [d]^T \{T\} + [\epsilon]\{E\}
\tag{2.11}
$$

The explicit form of these equations, for both the actuation and the sensing modes are given in the next subsections.

### 2.2.2. ACTUATION MODE

The explicit form of the equation for actuation mode is shown in equation 2.12 .

$$
\begin{Bmatrix} S_{11} \\ S_{22} \\ S_{33} \\ 2S_{23} \\ 2S_{31} \\ 2S_{12} \end{Bmatrix}
=
\begin{bmatrix}
s_{11} & s_{12} & s_{13} & 0 & 0 & 0 \\
s_{12} & s_{22} & s_{23} & 0 & 0 & 0 \\
s_{13} & s_{23} & s_{33} & 0 & 0 & 0 \\
0 & 0 & 0 & s_{44} & 0 & 0 \\
0 & 0 & 0 & 0 & s_{55} & 0 \\
0 & 0 & 0 & 0 & 0 & s_{66}
\end{bmatrix}
\begin{Bmatrix} T_{11} \\ T_{22} \\ T_{33} \\ T_{23} \\ T_{31} \\ T_{12} \end{Bmatrix}
+
\begin{bmatrix}
0 & 0 & d_{31} \\
0 & 0 & d_{32} \\
0 & 0 & d_{33} \\
0 & d_{24} & 0 \\
d_{15} & 0 & 0 \\
0 & 0 & 0
\end{bmatrix}
\begin{Bmatrix} E_1 \\ E_2 \\ E_3 \end{Bmatrix}
\tag{2.12}
$$

Piezoelectric elements can be used in different actuation modes, depending on the topology and the direction of polarization in the piezoelectric material.

#### PIEZO STACK ACTUATOR

In figure 2.13, a piezo stack actuator is shown. In this configuration, multiple actuators with an opposite direction of polarization are stacked to produce a higher displacement. This type of actuator depends on the $d_{33}$ coefficient. This means that when an electric field is applied on the structure, it will extend in the same direction.

#### PIEZO SHEAR ACTUATOR

In figure 2.14, a piezo shear actuator is shown. This type of actuator depends on the $d_{15}$ coefficient. This means that when an electric field is applied on the structure, it will have a shear deflection as shown in figure 2.14.
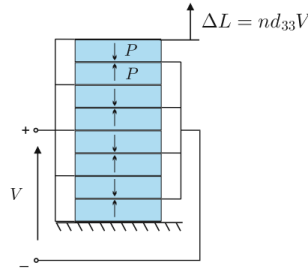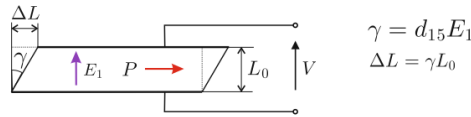
Figure 2.13: Piezo stack actuator [1]



Figure 2.14: Piezo shear actuator [1]

Another possible actuation mode for piezoelectric materials is the bending mode. A thin layer of piezoelectric material is attached to the surface of a flexible structure. When voltage is applied in the polarization direction, the piezoelectric transducer will extend in the longitudunal direction (or contract, depending on input voltage). This type of actuation mode is shown in figure 2.15.

Because the piezoelectric transducer is bonded to the beam, the extension of the piezoelectric transducer results in the strain distribtion in the beam shown in figure 2.16

When a pure bending moment is applied at a beam, the induced strain distribution is similar to figure 2.16 [10]. So, this type of actuator induces bending and is therefore referred to as 'piezoelectric bending actuator'.

Figure 2.17 shows that for modelling purposes, a rectangular piezoelectric bending transducer could be modelled as two opposing bending moments at each end of the transducer.

In AVC, often bending modes of a flexible system are of interest. For these situations, it is the most logical option to counter these bending modes by applying bending moments at specific locations on the flexible structure. Therefore, piezoelectric bending actuators are ideally suited to use in suppressing vibrations in beams [9].

## 2.2.3. Sensing mode

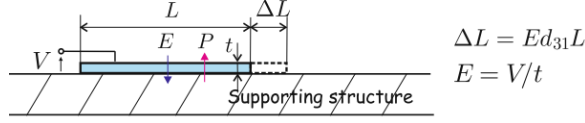The explict form of the equation for the sensing actuation mode is shown in equation 2.13.
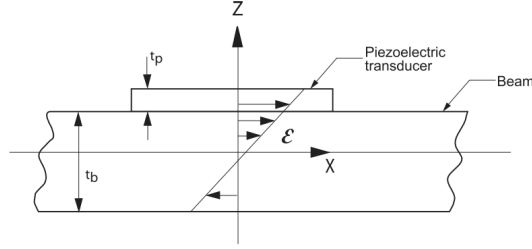
Figure 2.15: Piezo bending actuator [1]



Figure 2.16: Strain distribtion in beam caused by piezo bending actuator [9]

$$\left\{\begin{array}{c} D_1 \\ D_2 \\ D_3 \end{array}\right\} = \begin{bmatrix} 0 & 0 & 0 & 0 & d_{15} & 0 \\ 0 & 0 & 0 & d_{24} & 0 & 0 \\ d_{31} & d_{32} & d_{33} & 0 & 0 & 0 \end{bmatrix} \left\{\begin{array}{c} T_{11} \\ T_{22} \\ T_{33} \\ T_{23} \\ T_{31} \\ T_{12} \end{array}\right\} + \begin{bmatrix} \epsilon_{11} & 0 & 0 \\ 0 & \epsilon_{22} & 0 \\ 0 & 0 & \epsilon_{33} \end{bmatrix} \left\{\begin{array}{c} E_1 \\ E_2 \\ E_3 \end{array}\right\} \quad (2.13)$$

As explained in subsection 2.2.1, piezoelectric materials can be used in actuation mode (converse piezoelectric effect) and sensing mode (direct piezoelectric effect). Therefore, the actuators shown in figures 2.13 and 2.15 could also be used as strain sensors. In the piezo bender configuration, the sensor would sense the strain parallel to the longitudunal direction of the transducer.

The generated charge in a piezoectric sensor can be determined from equation 2.14 [9].

$$q = \int\int \begin{bmatrix} D_1 & D_2 & D_3 \end{bmatrix} \begin{bmatrix} dA_1 \\ dA_2 \\ dA_3 \end{bmatrix} \quad (2.14)$$

where $dA_1$, $dA_2$ and $dA_3$ are the differential electrode areas in the 2-3, 1-3 and 1-2 planes respectively. The generated voltage is related to the charge via:

$$V_p = \frac{q}{C_p} \quad (2.15)$$

where $C_p$ is the capacitance of the piezoelectric sensor.

When the measured voltage $V_p$ is known, the strain can be determined by solving the integral shown in equation 2.14. Assuming that the strain is only in the 1-direction (the longitudunal direction of the piezoelectric transducer), the sensor voltage is found to be [9]:
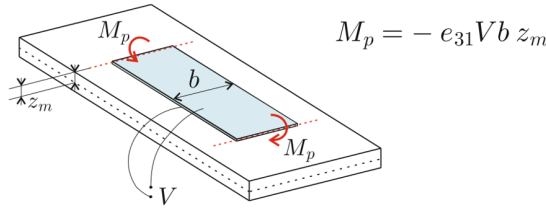
Figure 2.17: Model of piezo bending actuator [1]

$$V_s = \frac{d_{31}E_p w}{C_p} \int_l \epsilon_1 dx \qquad (2.16)$$

where $E_p$ is the Young's modulus of the sensor and $\epsilon_1$ is the average strain value over the sensors length. So, the average strain value over the piezoelectric transducers length could be obtained via equation 2.17.

$$\epsilon_1 = \frac{C_p V_s}{d_{31}E_p l w} \qquad (2.17)$$

However, equation 2.17 is only valid under the assumption that the sensor is only strained in the longitudunal direction. When this assumption is violated, which is often the case in real-life situations, equation 2.17 should be modified to equation 2.18.

$$\epsilon_1 = \frac{C_p V_s}{(1-v)d_{31}E_p l w} \qquad (2.18)$$

,

where $v$ is the Poisson's ratio of the material.

## 2.3. PLACEMENT OF PIEZOELECTRIC TRANSDUCERS

In order to use piezoelectric transducers as sensor and actuators in an AVC system, it is important to study the influence of the placement of these transducers on the damping performance. In state-of-the-art literature, different optimization criteria for finding the best possible locations of piezoelectric patches have been researched before. In the following subsection, the objective functions that are often used in literature will be discussed [11].

### 2.3.1. OPTIMIZATION CRITERIA

1. **Maximizing modal forces/moments**

   In active vibration control situations, it is desired that piezoelectric actuators strain the host structure in a direction opposite to the developed strains caused by vibration modes. An often used optimization criteria is 'maximizing modal forces/moments'. The modal force applied on a structure depends on the position of the actuator. When

**2**

a flexible plate is controlled with independent modal space control, the modal force applied by an actuator to excite the j-th mode is given by equation 2.19 [12].

$$Q_j(t) = -a_p b_p (\frac{h_s + h_p}{2}) L[\psi_j] V_j(t) \tag{2.19}$$

where $L = e_{31}\{(\frac{\partial^2}{\partial x^2}) + (\frac{\partial^2}{\partial y^2})\}$ for isotropic piezoelectric material. From equation 2.19, it can be concluded that the modal force is maximal when $L[\psi_j]$ is maximal. $L[\psi_j]$ is maximal at the locations where the sum of modal strains in x-direction and y-direction is maximal. For a 1-dimensional cantilever beam, the operator $L[\psi_j]$ is maximal at the location of maximal modal strain.

Therefore, it can be reasoned that the piezoelectric actuators should be placed at the locations with the highest modal strain. If the actuators would be placed at locations of zero strain, it would not even be able to strain the host structure at all. Similar to the actuators, sensors are also most effective when placed at the locations of high modal strain. Piezoelectric sensors can sense the average bending strain along the electrode surface. If the piezoelectric sensor would be placed at a strain node (a location with zero average modal strain) it would not be able to sense that specific mode.

2. **Maximizing deflection of the host structure**
   When an external voltage is applied to a piezoelectric actuator that is bonded to the surface, it will produce transverse deflections in the host structure. These transverse deflections are dependent on the placement of the piezoelectric actuator. Therefore, an often used optimization criterion for finding the optimal location of piezoelectric actuators is to maximize the transverse deflection of the host structure. Several examples where this criterium is used for to determine the optimal locations can be found in [13] [14] [15] [16].

By using the assumed mode shapes method, the dynamic transverse deflection of the beam with piezoelectric patches that are bonded to the surface is given by [17].

$$w(x, t) = \sum_{i=1}^{\infty} \psi_i(x)\eta_i(t) \tag{2.20}$$

The sensor output voltage is given by:

$$V_{\text{sensor}} = e_{31} b_p d \int_{x1}^{x2} \frac{\partial^2 w(x, t)}{\partial x^2} dt \tag{2.21}$$

$x_1$ and $x_2$ are the sensor begin and end points along the length of the beam. The optimal position of the actuator and sensor is where the beams transverse deflection is the highest. This corresponds with the location of maximum curvature, which corresponds with the location of highest modal strain. For the sensor, the optimal position is the position where the value of $V_{\text{sensor}}$ is maximal. It can be argued the function expressed in equation 2.21 has a maximal value when the expression in equation 2.22 is satisfied.

$$\frac{\partial^3 w(x, t)}{\partial x^3} = 0 \tag{2.22}$$

So, the optimal position of a collocated sensor-actuator pair is at the location where the third derrivative of the transverse displacement with respect to the coordinate along the beam is zero. This is at the location where the (modal) strain of the system is maximal [17].

3. **Minimizing control effort**
Another criterium that can be used to find the optimal location for placing piezoelectric sensors and actuators on a flexible structure, is to minimize the control effort. In active vibration control, external energy is used to cause deflection in the host structure. In the modal domain, the dynamic equations of motion are described by equation 2.23 [17].

$$\ddot{\eta}(t) + D\dot{\eta}(t) + \Lambda \eta(t) = B_a V_{\text{act}} \tag{2.23}$$

where $\eta$ is the modal amplitude. The modal amplitude is controlled by external voltage $V_{\text{act}}$. In state space, the system can be written as

$$\begin{aligned}\dot{X}(t) &= AX(t) + BV_{\text{act}} \\ Y(t) &= CX(t)\end{aligned} \tag{2.24}$$

where B = $\begin{bmatrix} 0 \\ B_a \end{bmatrix}$ and C = $\begin{bmatrix} 0 & B_v \end{bmatrix}$.

Electrical energy spent in active vibration control is dependent on the placement of the actuator [18].

$$J_e = \int_0^\infty V_{\text{act}}^T R V_{\text{act}} dt \tag{2.25}$$

Minimization of the electrical energy spent is a method to find the optimal placement of the piezoelectric patches. This optimization will result in the actuator placement at areas of high modal strain in the flexible structure. [19]

4. **Maximizing degree of controllability**
Regardless of the control algorithm that will be used, a necessary condition for effective AVC is that the system should be controllable. A closed-loop system is controllable if every state variable can be affected in such a way that causes it to reach a particular value within a finite amount of time. If one or more state variables can not be affected in this way, the system is uncontrollable [20].

The controllability of a system is a function of the system dynamics and the placement and number of actuators. The essential condition for controllability is that the controllability matrix R must have full rank.

$$R = \begin{bmatrix} B & AB & A^2B & A^3B & ..... & A^{2n-1}B \end{bmatrix}_{1x2n}$$

The check of the rank of the controllability matrix only gives the information if the system is controllable or not. The degree of controllability does depend on the placement of sensors and actuators. At the optimal locations of the sensors and actuators, the degree of controllability of the system is at its maximum.

The degree of controllability can be expressed by using the controllability Gramian matrix '$G_c$' [21]. The expression for this matrix is shown in equation 2.26.

$$G_c(t) = \int_0^{t_1} e^{At} BB^T e^{A^T t} dt \qquad (2.26)$$

The effects of the placement of the actuators are contained in $G_c$ via the matrix $B$. To control each mode individually by applying minimal control effort, each diagonal term of $G_c$ should be maxmized. The performance index should then be [22]:

$$J_c = \max\{(G_c)_{11}, (G_c)_{22}, \ldots, (G_c)_{nn}\} \qquad (2.27)$$

The degree of controllability can be used as a method to determine the optimal location of the actuators. For example, this is used by [23], [24] and [25].

5. **Maximizing degree of observability**
   Observability is another necessary condition for AVC. A closed-loop system is completely observable if the system output contains information about each of the state variables. If one or more state variables can not be observed, the system is unobservable [20]. The standard check for the observability is to test the rank of the observability matrix O:

$$O = \begin{bmatrix} C & CA & CA^2 & CA^3 & \ldots & CA^{2n-1} \end{bmatrix}_{1x2n}^T$$

Similar to the controllability problem, the rank check of the observability also only tells if the system is observable or not. To find out what is the optimal location for the placement of the sensors, the observability Gramian matrix $G_o$ is defined [21].

$$G_o(t) = \int_0^\infty e^{At} CC^T e^{A^T t} dt \qquad (2.28)$$

The effects of the placement of the sensor are contained in $G_o$ via the matrix $C$. Information about the degree of observability of a system is hidden in the eigenvalues of the observability Gramian matrix. If a certain eigenvalue is small, it means that the eigenmode corresponding to this eigenvalue is not well observed. To maximize the global observability of a system, maximization of criterion 2.29 is proposed by [21].

$$J_o = \text{tr}\begin{bmatrix} G_o \end{bmatrix} * (G_o)^{1/2n} \qquad (2.29)$$

If the goal is to maximize the observability of each mode individually, the diagonal terms of $G_0$ should be maximized [22].

$$J_o = \max\{(G_o)_{11}, (G_o)_{22}, ....., (G_o)_{nn}\} \tag{2.30}$$

The degree of observability can be used as a method to determine the optimal location of the sensors. In literature, this is used by for example [23] and [24].

In systems where the sensors and actuators are collocated, the measure of modal contrallability and modal observability are equivalent. This means that for collocated systems, the optimal locations of the sensor are similar to the optimal locations of the actuator [24].

The optimization methods 'maximizing modal forces/moments', 'maximizing deflection' and 'minimizing control effort' as explained above all suggest that placing actuators and sensor at locations with largest modal strain is the most efficient strategy. Also, it has been shown that systems are both controllable and observable if the sensors and actuators are placed at locations with high deformation/strain. So, when collocated sensor actuator pairs are placed in a location where the modal strain is high, it can efficiently be used to suppress the corresponding mode. Therefore, in this research, sensors and actuators will be placed at locations with high modal strain.

## 2.4. NUMERICAL SIMULATION

To verify the findings from section 2.3, an Euler-Bernouilli finite element model was made for the flexible cantilever beam. The goal of this simulation is to see what happens when the piezoelectric patches are located at the optimal location (so at the modal strain maxima), and how the performance changes if the patches are placed at other locations. In this section, the numerical model will be explained, and finally the findings will be discussed.

### 2.4.1. NUMERICAL MODEL

The equation of motion for the cantilever beam is given by:

$$\mathbf{M}\ddot{\mathbf{u}} + \mathbf{C}\dot{\mathbf{u}} + \mathbf{K}\mathbf{u} = \mathbf{f} \tag{2.31}$$

where $\mathbf{u}$ is the vector that describes the vertical translation and the rotation of every node and $\mathbf{f}$ is the vector that describes the applied forces and moments at every node of the beam.

$$\mathbf{u} = \begin{bmatrix} u_1 \\ \theta_1 \\ u_2 \\ \theta_2 \\ . \\ . \\ . \\ u_N \\ \theta_N \end{bmatrix}, \mathbf{f} = \begin{bmatrix} F_1 \\ M_1 \\ F_2 \\ M_2 \\ . \\ . \\ . \\ F_N \\ M_N \end{bmatrix}$$

$\mathbf{M}$ is the mass matrix of a single element and depends on the length of the element, the density of the beam material and the cross-sectional area of the beam. $\mathbf{K}$ is the stiffness matrix of a single element and depends on the Youngs modulus of the beam material, the length of one element and the cross-sectional area of the beam.
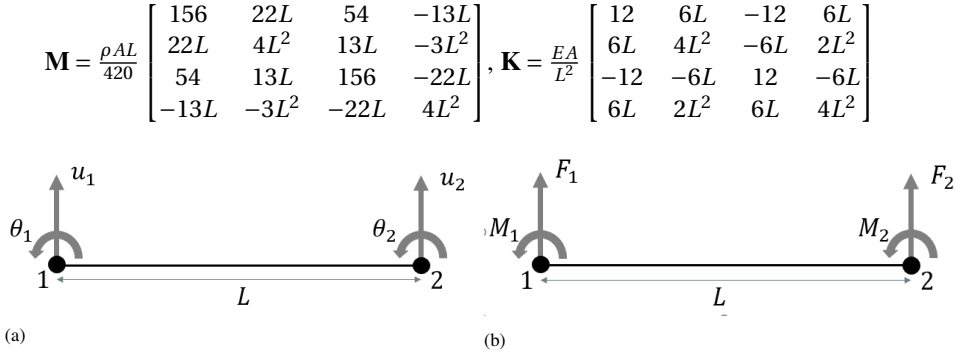
$$\mathbf{M} = \frac{\rho A L}{420} \begin{bmatrix} 156 & 22L & 54 & -13L \\ 22L & 4L^2 & 13L & -3L^2 \\ 54 & 13L & 156 & -22L \\ -13L & -3L^2 & -22L & 4L^2 \end{bmatrix}, \mathbf{K} = \frac{EA}{L^2} \begin{bmatrix} 12 & 6L & -12 & 6L \\ 6L & 4L^2 & -6L & 2L^2 \\ -12 & -6L & 12 & -6L \\ 6L & 2L^2 & 6L & 4L^2 \end{bmatrix}$$



Figure 2.18: Euler-Bernouilli FEM element. (a) degrees of freedom; (b) forces and moments
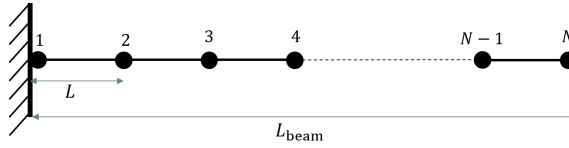


Figure 2.19: N elements combined to cantilever beam

To analyse the frequency response of the cantilever beam without any additional damping patches, equation 2.31 is transformed into the frequency domain. Also, the modal damping ratio $\mathbf{C} = \eta \mathbf{K}$ is used where $\eta$ is the modal damping ratio (typically around 1%.) The equation of motion in frequency domain is given by equation 2.32.

$$(-\omega^2 \mathbf{M} + j\omega\eta\mathbf{K} + \mathbf{K})\mathbf{u}(\omega) = \mathbf{f}(\omega) \tag{2.32}$$

The first step is to check if this model gives results that are comparable to a COMSOL finite element analysis and to the eigenfrequencies that can be calculated in an anlytical way.

To analyse the frequency response of the cantilever beam, a force is applied at the end node. This force is present among the entire frequency range. The frequency is swept from approximately 0.1 to 300 Hz (so that it captures the first 4 bending modes) and the response of the system is computed for every frequency step. Then, the magnitude of the displacement of the end node and its phase are plotted to form the frequency response function. The result (with number of elements N=100) is shown in figure 2.20.

Now, the eigenfrequencies of the first four modes of this model can be compared with eigenfrequencies of the COMSOL finite element model and the analytical calculation to check if this Euler-Bernouilli model is valid.

The analytical calculation of the eigenfrequencies is obtained from the book Formulas for Dynamics, Acoustics and Vibration [26]. The equation that is used is shown in equation 2.33.

$$f_i = \frac{\lambda_i^2}{2\pi L^2} \sqrt{\frac{EI}{\rho A}} \tag{2.33}$$
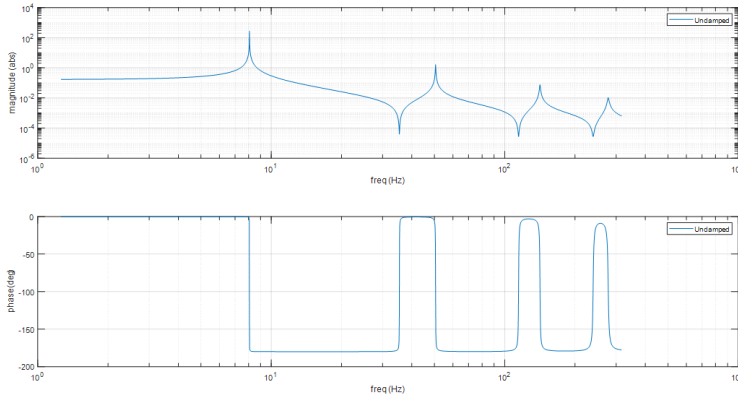
Figure 2.20: Frequency Response Function of Euler-Bernouilli beam

Where $\lambda_1 = 1.87510407$, $\lambda_2 = 4.69409113$, $\lambda_3 = 7.85475744$ and $\lambda_4 = 10.99554073$.

| Method | $f_1$ (Hz) | $f_2$ (Hz) | $f_3$ (Hz) | $f_4$ (Hz) |
|---|---|---|---|---|
| Euler-Bernoulli (N = 100) | 8.07 | 50.5 | 141.4 | 277.5 |
| $f_i = \frac{\lambda_i^2}{2\pi L^2} \sqrt{\frac{EI}{\rho A}}$ (eq. 2.33) | 8.06 | 50.5 | 141.5 | 277.3 |
| COMSOL (3D) | 8.17 | 51.2 | 143.5 | 281.5 |

Table 2.1: Eigenfrequency comparison of different computation methods

In table 2.1, the eigenfrequencies found by different methods are shown. It can be observed that the Euler Bernouilli method gives almost identical values as the method from [26]. Also, the COMSOL 3D FEM model gives fairly similar results. Therefore, it is assumed that the Euler-Bernouilli model is correct so far.

Now, this finite element model will be used to study the influence of the placement of the piezoelectric transducer on the damping performance. Every piezoelectric patch will have a specific mode of interest, that is the mode that has a peak strain value at the location of this piezoelectric patch. The objective is to maximize the influence of the piezoelectric actuator on the suppression of this specific mode. Therefore, as an example, the damping patch for mode 2 will be analysed and the influence of its location will be studied. In the next subsection, this simulation will be explained.

### 2.4.2. INFLUENCE OF DAMPING PATCH PLACEMENT

In the simulation, a cantilever beam will be excited by a force applied at the end node that is present at all frequencies. The piezoelectric transducer that will be used for the active vibration control of the mode of interest is added to the Euler-Bernouilli model. In figure 2.17, it is shown that a rectangular piezoelectric transducer that is used as an actuator can be modelled as two opposing bending moments at the ends of the transducer. This is implemented in the model that is schematically shown in figure 2.21. To study the

influence of this piezoelectric transducer specifically on mode 2, the bending moments are only applied at frequencies close to the resonance frequency of mode 2. The magnitude of the opposing bending moments as shown in figure 2.20 is kept constant, and the length of the transducer is kept constant as well (chosen as 10% of the beam length). To study how the frequency response of the system changes when the location of the piezoelectric transducer is changed, the variable $x_{piezo}$ as shown in figure 2.21 will be varied an the influence on the frequency response of the tip of the beam will be studied.
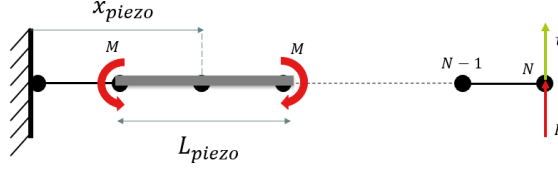


Figure 2.21: Model used for study of optimal placement of piezoelectric transducer

In figure 2.22, the frequency response of the systemwithout the damping patch is shown in blue, and the system where the damping patch is modelled as two opposing bending moments (at an arbitrary value of $x_{piezo}$) is shown in orange. It can be seen that the magnitude of the resonance peak is lower in the system where the damping patch is applied. To study the influence of the location of the piezoelectric transducer on the frequency response, the reduction of the damping peak is computed for different values of $x_{piezo}$.



(a)

(b)
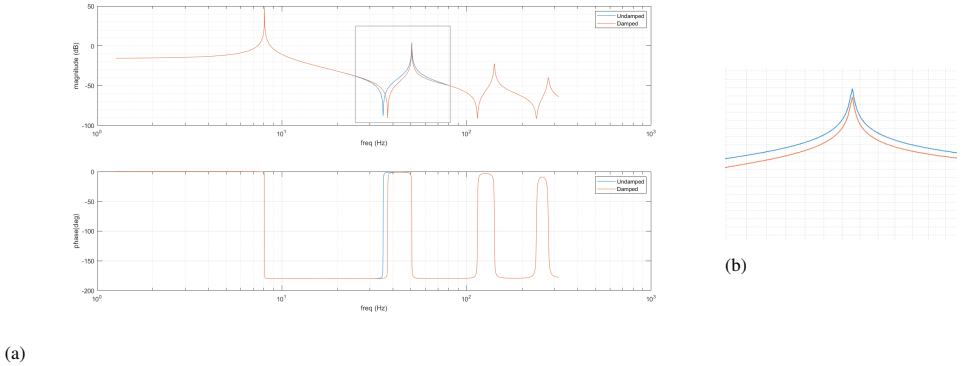
Figure 2.22: Frequency response of system described in figure 2.21 (a) complete FRF; (b) Zoomed-in at mode 2

Now, the location of the piezoelectric $x_{piezo}$ is varied and the reduction of the resonance peak is computed. The result of this study is shown in figure 2.23, where the normalized reduction of the magnitude of the resonance peak is shown for different values of $x_{piezo}$.

From figure 2.23, it can be seen for a value of $x_{piezo} = 0.53 L_{beam}$, the reduction of the magnitude of the resonance peak is maximal. This exactly corresponds to a peak value of the modal strain of mode 2, which can be seen in figure 2.24 where the modal strain and displacement of mode 2 are shown.

So, this numerical example verified the findings from section 2.3 are correct. This
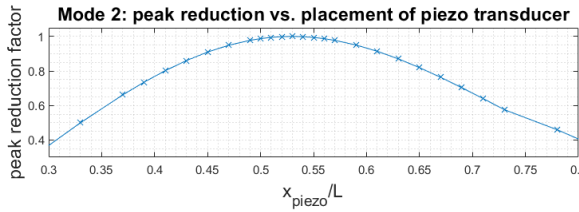
Figure 2.23: Reduction of resonance peak of mode 2 vs. piezoelectric transducer location



(a)                                                                (b)
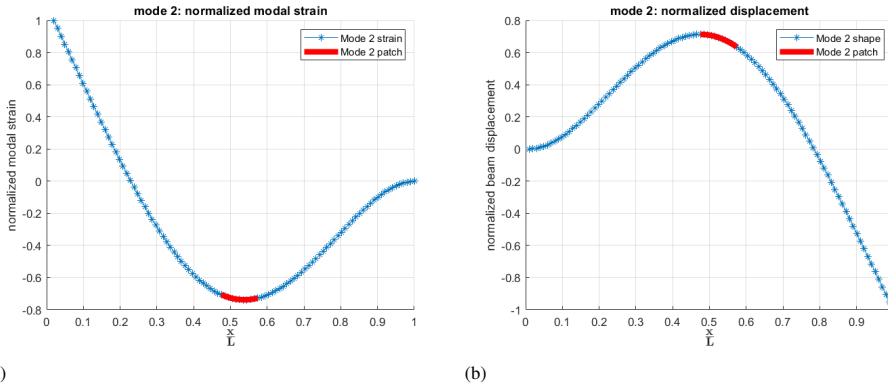
Figure 2.24: Optimal location of damping patch of mode 2: (a) Normalized strain; (b) Normalized displacement

means that if the objective is to maximize the controllability of a specific mode, the optimal location to place a piezoelectric actuator is at the modal strain peak.

This procedure has also been carried out for other modes of interest, and similar results are obtained. So, from both literature and simulations it can be concluded that placing piezoelectric transducers at locations with high modal strain leads to a high controllability of that specific mode.

## 2.5. RECENT RESEARCH ON OVER-ACTUATION IN AVC

To the best of the writers knowledge, in all of the work present in state-of-the art scientific literature distributed over-actuation and over-sensing has not been studied. The recent work done by [27] was the first study that included distributed over-actuation in an AVC system. In this work, it was showed that an AVC system that uses distributed over-actuation has significant benefits in terms of damping performance compared to 'traditional' AVC systems, where the number of actuators is less than or equal to the number of modes to be controlled. From this work, it can be conlcuded that high-tech precision machines will benefit from using distributed over-actuation to actively damp vibrations in the flexures.

Figures 2.25a and 2.25b show the perfect-actuated and over-actuated setups respectively.

For clarity, side views of these two different experimental setups are shown in figures 2.26 and 2.27.

(a)

(b)
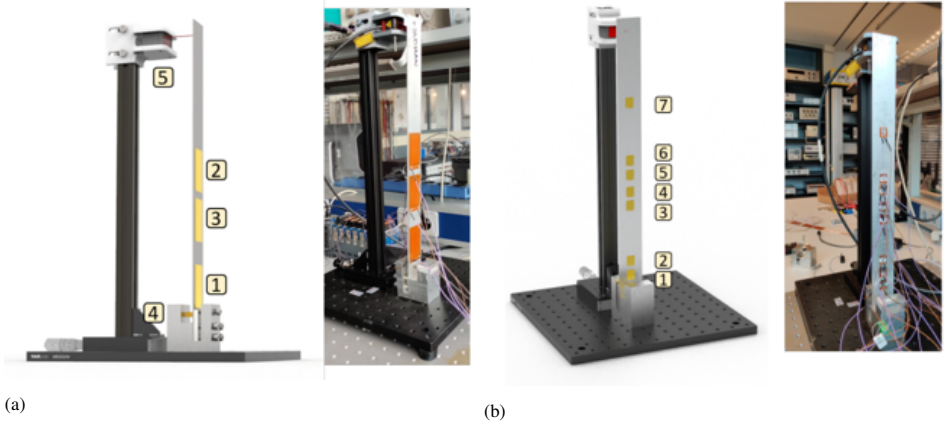
Figure 2.25: Experimental setup of [27] (a) Perfect-actuated case; (b) Over-actuated case
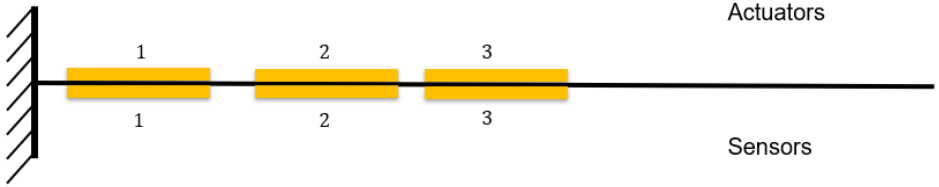


Figure 2.26: Schematic side view of setup with over-actuation and perfect-sensing

In the case-1 setup (figure 2.26), 3 collocated sensor/actuator pairs are used to suppress the first 3 vibration modes of a flexible beam. The system identification resulted in a 3x3 frequency response function from the piezo actuators to the piezo sensors. The controller was tuned based on the diagonal elements of this 3x3 FRF. So, this means that the setup for case-1 was purely decentralized (as explained in section 2.1). The transfer function from the sensor to its corresponding collocated actuator was used to tune the controller that sends the voltage input to that specific actuator.

This was not the case in the case-2 setup that is shown in figure 2.27. In this figure, 7 actuators and 3 sensors were used to control the first 3 vibration modes of a cantilever beam. So, the system identification will result in a 7x3 transfer function from the actuators to the sensors. When this setup is compared to figure 2.7, it can be concluded that the case-2 setup is not fully decentralized, and the benefits explained in section 2.1 are not fully valid for this system.

Also, the controller can not be tuned based on the diagonal elements of the 7x3 FRF function in the way that was done in the case-1 setup. This means that the controller that sends a voltage signal to a specific actuator can not be tuned based on the strain data at the exact location of this actuator. Actuator 7 could not even be used at all because of the non-collocation. While the case-2 setup did show significant improvement of the damping perfomance, the literature suggests that a setup where the sensors are distributed as well
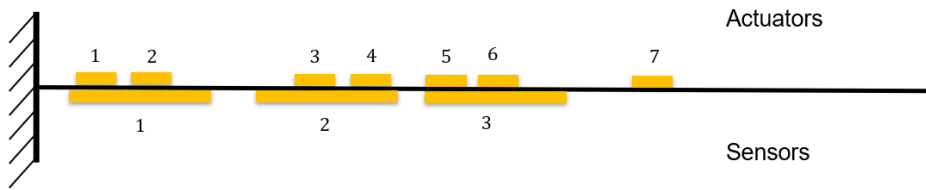
Figure 2.27: Schematic side view of setup with over-actuation and perfect-sensing

would be even better. If over-sensing would be added to the system on top of over-actuation, the result would be a fully collocated system of which the controllers could be optimally tuned by using the diagonal elements of its frequency response function. Because the sensors allow for better tuning of the controllers and thus more optimal control inputs to the actuators, it is expected that a system with both over-sensing and over-actuation will result in an even better damping performance. Also, the weight of the total damping system will be lower if multiple small sensors are used instead of a few larger sensors.

# REFERENCES

[1] A. Preumont. *Vibration Control of Active Structures: An Introduction.* Solid Mechanics and Its Applications. Springer, 2013. ISBN 9789400720336.

[2] Preumont, A., François, A., De Man, P., & Piefort, V. (2003). Spatial filters in structural control. *Journal of sound and vibration*, 265(1), 61-79.

[3] Mariantonieta Gutierrez Soto and Hojjat Adeli. Multi-agent replicator controller for sustainable vibration control of smart structures. *Journal of Vibroengineering,* 19(6): 4300–4322, sep 2017. doi: 10.21595/jve.2017.18924. URL https://doi.org/10.21595%2Fjve.2017.18924.

[4] Jan Lunze. *Feedback control of large scale systems*. Prentice Hall PTR, 1992.

[5] Vahab Nekoukar and Abbas Erfanian. A decentralized modular control framework for robust control of fes-activated walker-assisted paraplegic walking using terminal sliding mode and fuzzy logic control. *IEEE transactions on biomedical engineering,* 59(10):2818–2827, 2012.

[6] Ugur Aridogan and Ipek Basdogan. A review of active vibration and noise suppression of plate-like structures with piezoelectric transducers. *Journal of Intelligent Material Systems and Structures*, 26(12):1455–1476, 2015.

[7] Jayant Sirohi and Inderjit Chopra. Fundamental understanding of piezoelectric strain sensors. *Journal of intelligent material systems and structures,* 11(4):246–257, 2000.

[8] Goran Barac. Multimode damping with activated metamaterials. *Master Thesis TU Delft,* 2020.

[9] SO Reza Moheimani and Andrew J Fleming. *Piezoelectric transducers for vibration control and damping.* Springer Science & Business Media, 2006.

[10] RC Hibbeler. *Mechanics of Materials Ninth Edition.* Pearson Education, Inc, 2014.

[11] Vivek Gupta, Manu Sharma, and Nagesh Thakur. Optimization criteria for optimal placement of piezoelectric sensors and actuators on a smart structure: a technical review. *Journal of Intelligent Material Systems and Structures*, 21(12):1227–1243, 2010.

[12] Li Bin, Li Yugang, Yin Xuegang, and Huang Shanglian. Maximal modal force rule for optimal placement of point piezoelectric actuators for plates. *Journal of Intelligent Material Systems and Structures,* 11(7):512–515, 2000.

[13] JC Bruch Jr, JM Sloss, S Adali, and IS Sadek. Optimal piezo-actuator locations/ lengths and applied voltage for shape control of beams. *Smart Materials and Structures,* 9(2):205, 2000.

[14] M Sunar, SJ Hyder, and BS Yilbas. Robust design of piezoelectric actuators for structural control. *Computer methods in applied mechanics and engineering,* 190 (46-47):6257–6270, 2001.

[15] Victor M Franco Correia, Cristóvão M Mota Soares, and Carlos A Mota Soares. Refined models for the optimal design of adaptive structures using simulated annealing. *Composite Structures,* 54(2-3):161–167, 2001.

[16] José M Simoes Moita, Victor M Franco Correia, Pedro G Martins, Cristovao M Mota Soares, and Carlos A Mota Soares. Optimal design in vibration control of adaptive structures using a simulated annealing algorithm. *Composite Structures,* 75(1-4):79– 87, 2006.

[17] Jingjun Zhang, Lili He, Ercheng Wang, and Ruizhen Gao. A lqr controller design for active vibration control of flexible structures. *In 2008 IEEE Pacific-Asia Workshop on Computational Intelligence and Industrial Application*, volume 1, pages 127–132. IEEE, 2008.

[18] Tae-Woo Kim and Ji-Hwan Kim. Optimal distribution of an active layer for transient vibration control of a flexible plate. *Smart Materials and Structures,* 14(5):904, 2005.

[19] K Ramesh Kumar and S Narayanan. Active vibration control of beams with optimal placement of piezoelectric sensor/actuator pairs. *Smart Materials and Structures,* 17 (5):055008, 2008.

[20] Daniel J Inman. *Vibration with control.* Wiley Online Library, 2006.

[21] A Hác and L Liu. Sensor and actuator location in motion control of flexible structures. *Journal of sound and vibration,* 167(2):239–261, 1993.

[22] Isabelle Bruant and Laurent Proslier. Optimal location of actuators and sensors in active vibration control. *Journal of intelligent material systems and structures*, 16(3): 197–206, 2005.

[23] Isabelle Bruant, Laurent Gallimard, and Shahram Nikoukar. Optimal piezoelectric actuator and sensor location for active vibration control, using genetic algorithm. *Journal of Sound and Vibration,* 329(10):1615–1635, 2010.

[24] Zhi-cheng Qiu, Xian-min Zhang, Hong-xin Wu, and Hong-hua Zhang. Optimal placement and active vibration control for piezoelectric smart flexible cantilever plate. *Journal of Sound and Vibration,* 301(3-5):521–543, 2007.

[25] Zorić, N. D., Simonović, A. M., Mitrović, Z. S., & Stupar, S. N. (2013). Optimal vibration control of smart composite beams with optimal size and location of piezoelectric sensing and actuation. *Journal of Intelligent Material Systems and Structures*, 24(4), 499-526.

[26] Robert D. Blevins. John Wiley and Sons, 2016. ISBN 978-1-119-03811- 5. URL https://app.knovel.com/hotlink/toc/id:kpFDAV0001/ formulas-dynamics-acoustics/formulas-dynamics-acoustics.

[27] Madhan Gopal Muruganandam Mallur. A comparative study on distributed active damping of flexible systems. *Master Thesis TU Delft*, 2020.

[28] P. Shivashankar and S. Gopalakrishnan. Review on the use of piezoelectric materials for active vibration, noise, and flow control. *Smart Materials and Structures,* 29(5):053001, 2020.

**2**

# 3

# ACTIVE VIBRATION CONTROL: USING OVER-SENSING AND OVER-ACTUATION

**T.K. van der Graaf, M.B. Kaczmarek, S.H. HosseinNia**

***ABSTRACT*** *The demand for faster production times and higher precision in the industrial automation is ever-increasing. Resonance modes caused by flexural elements in these machines are limiting the maximum bandwidth. To improve the performance of these machines, an active vibration control (AVC) system is needed. In present scientific literature, all AVC systems consist of an under-actuated or perfect-actuated setup. The damping performance of these systems could be increased by implementing an over-actuated setup. By using over-actuation, control inputs for suppressing modes can be provided at more efficient locations. This increases the amount of damping. In this paper, an over-actuation and over-sensing strategy for active damping is proposed. In this new method, a large number of piezoelectric sensors and actuators are used to control the first four vibration modes of a cantilever beam. The damping performance is evaluated in an experimental setup. Finally, the performance of the new topology of sensors and actuators is compared to the state-of-the-art active damping method that uses a perfect-actuation strategy. The improvement of the new method compared to the state-of-the-art method is shown both in time and frequency domain.*

**3** 

## 3.1. INTRODUCTION

Nowadays, the computational power of smartphones is a million times higher than the computational power of computers used in the first moon mission by NASA. These computers were approximately the size of a car and costed millions of dollars. Currently, a smartphone can be obtained for several hundred dollars and easily fits in your pocket. This development is in line with Moore's law, which states that the number of transistors in integrated circuits doubles approximately every 24 months [1]. To facilitate further developments, the performance of the machines in the high-tech must increase. The performance is related to the bandwidth of the machines. Therefore, it is tried to push the bandwidth as high as possible in the high-tech industry. However, the maximum achievable bandwidth of a system is limited by structural vibration modes.

Moreover, there is a trend in high-tech mechatronic systems to use compliant flexures instead of traditional joints. Flexures are beneficial because of their low friction, high repeatability and low maintenance requirements [2]. However, the introduction of compliant flexures into high-precision machines is problematic for the damping design of these systems. The low structural damping of flexural elements can cause multiple resonance modes to be excited. In consequence, large oscillations can occur. Furthermore, high-tech machines often operate in vacuum. Because of this, there is no viscous damping in the system. Thus, in order to limit the negative effects of the use of compliant flexures, a damping system is needed. A damping system is especially critical when the bandwidth of a system is limited by vibration modes. Schematic figures of different existing damping methods are shown in figure 3.1.



(a)                              (b)                              (c)
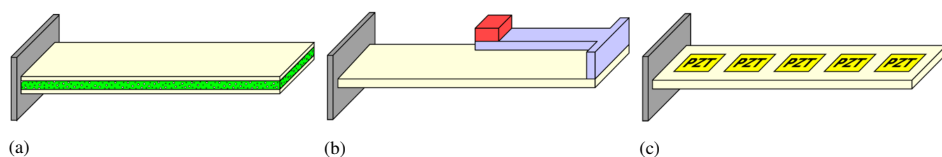
Figure 3.1: Schematic overview of different damping methods (a) Constrained Layer Damping; (b) Tuned Mass Damper; (c) Active Damping

Constrained layer damping and tuned mass damper are shown in figure 3.1a and 3.1b respectively. Both of these methods can be classified as passive damping as they use mechanical measures to suppress vibrations. While passive damping methods are effective to suppress a structural resonance, the damping to weight ratio is not optimal. The amount of damping is proportional to the added mass. Therefore, the added mass for suppressing multiple vibration modes will be too high. Also, passive damping methods are generally only effective in a narrow frequency range and not used for suppressing multiple modes.

Another existing damping method is active damping. A schematic illustration of active damping is shown in figure 3.1c. To suppress vibrations, sensors, actuators and a control algorithm are used. In active vibration control (AVC), piezoelectric transducers are often used as both sensors and actuators. In general, piezoelectric transducers are easy to integrate, cost effective, vacuum-proof and have a wide-frequency operation range [3]. Because of the wide-frequency operation range of the transducers, active damping can be used to suppress multiple resonance modes.

The primary objective of the controller in AVC is to increase the negative real part of the system poles, while maintaining the natural frequencies essentially unchanged [3]. Increasing the negative real part of the poles will reduce the magnitude of the resonance peaks in the frequency response function. The role of damping in a system is shown in figure 3.2. This figure illustrates both the pole locations and the dynamic amplification plots of an AVC system.
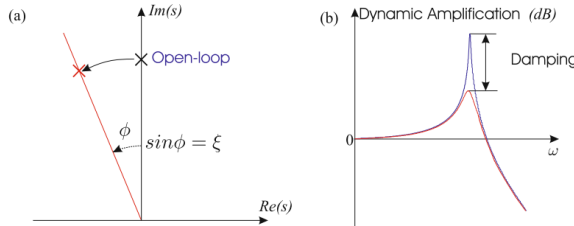


Figure 3.2: Role of Damping [3] (a) System poles, (b) Dynamic amplification

Active damping is a well-studied topic. In general, there are two different structures of the control system: centralized control and decentralized control. In centralized control, data from different sensors (which are distributed along the host structure) is combined and one output is computed. The result of this data combination could for example be the mode shapes and vibration amplitude.

In decentralized control however, the control problem is divided into a set of smaller subsystems. The data of different sensors is not combined and the system will consist of a number of collocated actuator/sensor pairs that each form an individual control loop.

In a decentralized system, all of the computations for the individual control loops can be performed in parallel. This will add to the reliability of the system significantly [4], because only part of the feedback system will stop working when there is an operational failure in one of the controllers.

When the decentralized and centralized control methods are compared, decentralized control has increased robustness, reduced complexity, reduced communication and a higher computational efficiency [4] [5]. For these reasons, decentralized control will be used in this reasearch.

Within decentralized AVC, the distribution of sensors and actuators can in general be divided into three categories: under-actuation, perfect-actuation and modal actuation. In the next part of the introduction, these categories will be explained. Furthermore, examples from the implementation of these methods will be given.

### UNDER-ACTUATION AND UNDER-SENSING

In under-actuation, the number of actuators is lower than the number of controlled modes. Similarly, in under-sensing, the number of sensors is lower than the number of controlled modes. In an under-actuated system, the control algorithm is designed in such a way that one actuator is used to control multiple modes. In literature, numerous examples of under-actuation and under-sensing in AVC are mentioned. For example, in a study performed by Bruant & Poselier, 1 sensor and 2 actuators were used to control the first 3 modes [6]. Other examples of under-actuated designs are the works of Daraji et al [7] and Zoric et al [8]. In

the study performed by Daraji et al, four actuator-sensor pairs for controlling 6 modes and the setup of the study performed by Zoric et al utilizes 4 actuator-sensor pairs for the first 5 modes. In all of these three studies, vibrations could effectively be damped to a certain extent.

## PERFECT-ACTUATION AND PERFECT-SENSING

In perfect-actuation and perfect-sensing, the number of actuators and sensors is equal to the number of modes to be controlled. In this way, each actuator-sensor pair is used to target one specific mode. This means that the actuators and sensors could be placed at an optimal location for the intended mode. An example of a study where perfect-actuation and perfect-sensing is implemented is the work of Lu et al, where 2 actuators are used for controlling 2 modes [9]. Another example is the work of Kumar et al [10]. In this work, 5 actuator-sensor pairs are used to target the first 5 vibration modes.

## PERFECT-ACTUATION VS. UNDER-ACTUATION

When the damping performance of under-actuated systems is compared to the performance of perfect-actuated systems, it can be concluded that the performance of perfect-actuated systems is higher. In under-actuation, a trade-off is made for the placement of the actuator, as it can not be placed at the optimal location for all of the modes of interest. This is not the case for perfect-actuation, because each mode is damped by an individual actuator. Therefore, the actuators can be placed at the most efficient location for the mode of interest.

## MODAL ACTUATION AND MODAL SENSING

In contrast to the under-actuation and perfect-actuation, it is also possible to design sensors and actuators that are only sensitive to one specific mode of interest. In 1990, the idea of modal sensors and modal actuators was first presented [11]. The concept of modal sensing and modal actuation is based on the principle of orthogonality of mode shapes. A modal filter can be obtained in two ways, continuous and discrete. Both of these methods will be explained in this section.

## CONTINUOUS MODAL FILTER

In a continuous modal filter, both the poling profile in the piezoelectric material and the profile of the surface electrodes need to be tailored to match the modal strain distribution. An example of a continuous modal filter is shown in figure 3.3. In this figure, the first two vibration modes of a cantilever beam are shown. The surface electrode profiles are designed to match the modal strain distribution. So, the modal filter on the left should be able to only actuate (or sense if it is used as sensor) the first mode, while the modal filter on the right can only actuate mode 2. Because of the orthogonality principle, other modes will not be excited by perfect modal actuators [3].

Although continuous modal filters are perfectly able to actuate and sense specific modes, practical implementation is a problem. Especially when multiple modes need to be damped, using continuous modal filters becomes almost impossible. For example, in a situation where the first four resonance modes are of interest, four modal sensors and four modal actuators need to be used. This means that the modal filters need to be stacked in some way, which is hard to realize in a physical system.
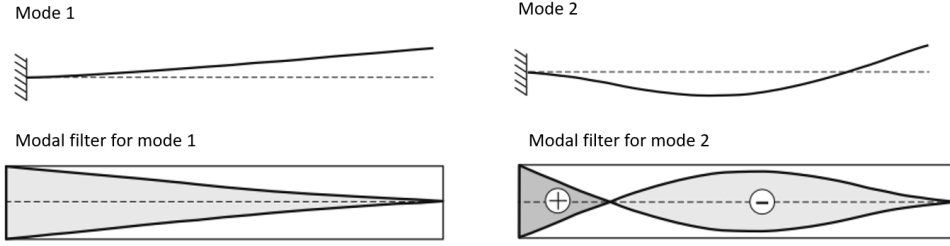
Figure 3.3: Continuous modal filter for the first two modes of a cantilever beam [3]

### DISCRETE MODAL FILTER

The other way of modal filtering is by implementing a discrete modal filter. In a discrete modal filter, an array of sensors (or actuators) is evenly distributed along the host structure. By applying weighting factors to each of the individual sensors, a continious modal filter could be mimicked to a certain extent. The weighting factor corresponds to the mode shape of the host structure. In discrete modal filtering, one sensor element can be used for different modes. Figure 3.4a shows the general structure of a discrete modal filter. An example of the weighting coefficients of a modal filter for the first four modes of a clamped-clamped plate with a grid of 4x8 regularly spaced sensors is shown in figure 3.4b.



(a)

(b)
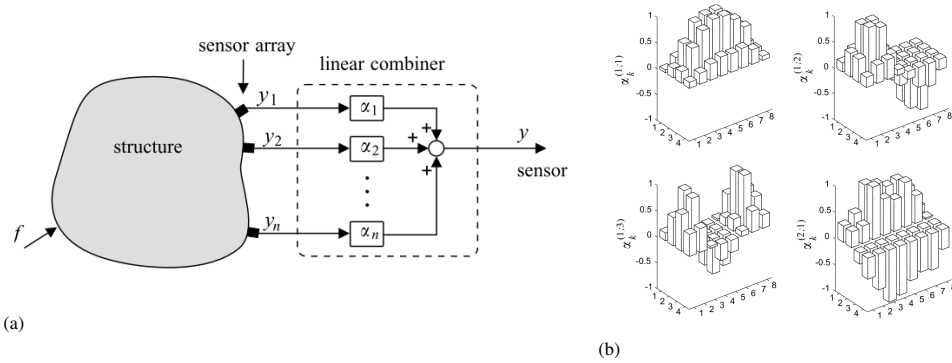
Figure 3.4: Discrete modal filter [12] (a) General Structure (b) Example of weighting coefficients of modal filter for the first four modes of a clamped-clamped plate

In literature, several studies that use a discrete modal filter can be found [12] [13]. In these studies, the discrete modal filter performed as an ideal modal filter up to a certain frequency. For higher frequencies, the wave number of one mode exceeds the number of regularly spaced sensors in that direction. This will cause spatial aliasing, as the sensor output appears as generated by a mode with a lower wave number. To get perfect modal filter behaviour up to high frequencies, the discrete sensor elements should be spaced as close as possible.

OVER-ACTUATION IN ACTIVE VIBRATION CONTROL

Besides the three well known and often used methods of under-actuation, pefect-actuation and modal actuation, there is another possible method called over-actuation. In over-actuation, the number of actuators is higher that the number of controlled modes.

The concept of using additional actuators has been researched extensively in motion systems for disturbance rejection. Steinbuch et al [14] proved that using additional actuators in motion control improves the modal controllability in the feedback path. The over-actuated design allows for additional actuators exclusively for controlling the resonances excited by the external disturbances while the other actuators are placed to get the desired motion.

Another study where over-acutation is considered is [15]. Here, eigenmodes of the structure are grouped. Then, a modal force is applied on the grouped modes. The control force is applied individually on each cluster of the control system. This strategy obtained a more energy efficient method for velocity control.

Another benefit of using an over-actuation and over-sensing strategy is robustness against failures. If one actuator or sensor fails, the performance will decrease but the system will still be damped by the other sensor-actuator pairs.

COMPARISON OF DIFFERENT METHODS

From state-of-the-art research, it can be concluded that using perfect-actuation results in a better damping performance than using under-actuation. However, it has been shown that implementing over-actuation can result in an even better performance [14] [15]. Also, continuous modal filters show ideal behaviours, but it is not practical to implement in physical systems where multiple modes are of interest. To a certain extent, continuous modal filters can be mimicked by using a discrete array of sensors and actuators and applying weighting factors to each discrete element. In a discrete modal filter, multiple transducers are used for one mode. Essentialy, a discrete modal filter can be seen as over-sensing (or over-actuation if the modal filter is an actuator). However, a discrete modal filter is an example of a centralized control system. For the reasons mentioned earlier, in this research a decentralized control system is preferred over a centralized control system. Therefore, a discrete modal filter will not be implemented in this study.

For studies that do use a decentralized control structure in AVC, under-actuation or perfect-actuation strategies are widely present in literature. In contrast, over-actuation has not been implemented in an AVC system before. This paper will propose a new topology for distributing sensors and actuators in AVC. The goal of this new topology is to improve the damping performance compared to the state-of-the-art methods. The system will have piezoelectric actuators and sensors that are distributed along a flexible cantilever beam. The actuator placement will be based on the modal strain distribution of the flexure. For mode 1 and 2, which have only 1 modal strain peak, actuators will be used at one location. For higher modes, actuators will be distributed at multiple modal strain peak locations. In this way, an over-actuated and over-sensed design will be realized for suppressing higher order modes. In the over-actuated design, the control force will be applied at more efficient locations. Therefore, the damping performance of the new system is expected to be better compared to systems that use perfect-actuation and perfect-sensing. If the new method of distributing sensors and actuators would be implemented in mechatronic systems, the bandwidth of these systems could increase. In the remainder of this paper, the proposed method

will be described in detail, and the damping performance will be tested experimentally on a flexible cantilever beam where the first four bending modes are considered. The reasons for design choices are explained in section 3.2 and a detailed description of the experimental setup is given in section 3.3. Then, the performance of the proposed method will be compared to the state-of-the-art perfect-sensing and perfect-actuation case in section 3.4.

## 3.2. DISTRIBUTION OF ACTUATORS AND SENSORS

To obtain the best possible damping performance, it is desired that the piezoelectric sensors and actuators are placed at the optimal location.

### 3.2.1. OPTIMAL PLACEMENT OF ACTUATORS AND SENSORS IN AVC

The optimal location for actuators in AVC is a well-studied topic in literature. Different optimization criteria can be used to find the optimal location of the actuators [16]. These optimization criteria and examples of studies where these criteria are used are:

- Maximizing modal forces/moments [17]

- Maximizing deflection of the host structure [18]

- Minimizing control effort [19]

- Maximizing controllability [20]

The optimization methods 'maximizing modal forces/moments', 'maximizing deflection' and 'minimizing control effort' all suggest that placing actuators and sensor at locations with largest modal strain is the most efficient strategy. Also, it has been shown that systems are both controllable and observable if the sensors and actuators are placed at locations with high deformation/strain. For systems with collocated sensors and actuators, the optimal location of the sensors is equal to the optimal location of the actuators [20]. So, when collocated sensor actuator pairs are placed in a location where the modal strain is high, it can efficiently be used to suppress the corresponding mode. Therefore, in this research, sensors and actuators will be placed at locations with high modal strain.

### 3.2.2. PLACEMENT OF ACTUATORS AND SENSORS ON CANTILEVER BEAM

In the previous subsection, it has been concluded that the optimal placement of sensors and actuators is at the location where the modal strain of the intended mode is maximal. However, higher order modes have multiple modal strain peaks. This can be seen in figure 3.5, where the modal strain distributions for the first 4 modes of a cantilever beam are visualized.

From figure 3.5, it can be observed that mode 3 has 2 peaks in the modal strain distribution, and mode 4 even has 3 peaks. Therefore, there are multiple efficient locations for actuator and sensor placement. Combining this with the findings of Steinbuch et al. [14], it can be concluded that for higher order vibration modes, the damping performance could improve by placing actuators at multiple locations. To get the benefits of a fully collocated system, the sensors should also be placed at the same locations. So, for modes that have multiple modal strain maxima, an over-actuated and over-sensed topology is expected to
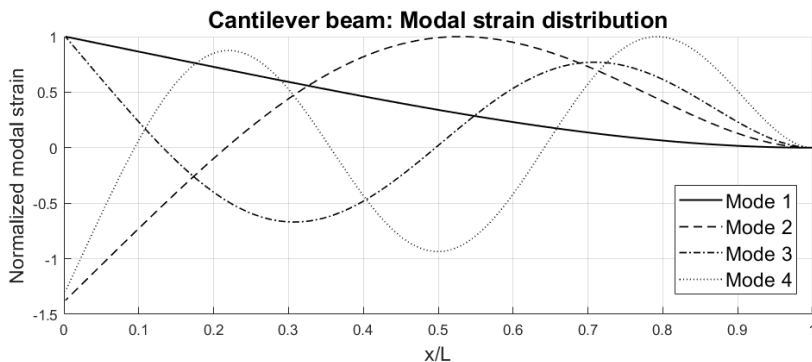
Figure 3.5: Modal Strain Distribution of first 4 bending modes of cantilever beam

have a better damping performance compared to perfecect-actuation and perfect-sensing topolgies.

## 3.3. METHOD

The damping performance of the proposed method that uses a over-actuation and over-sensing topology for higher order modes will be evaluated in an experimental test setup. To compare the perfomance of the proposed method with existing methods, experiments will be performed on different actuator and sensor layouts, and the resulting damping performance will be compared. The design of the experimental setup will be described in subsection 3.3.1. Then, the control algorithm is discussed in subsection 3.3.2. Finally, two different measurements that will be performed to evaluate the damping performance will be described in subsections 3.3.3 and 3.3.4.

### 3.3.1. DESCRIPTION OF EXPERIMENTAL SETUP

For the experimental setup, a flexible cantilever beam will be used. For simplicity, the system is analysed as one-dimensional, so only bending modes are considered. In this study, the first four modes are considered, which have resonance frequencies ranging from approximately 10 to 500 Hz.

To compare the damping performance of different distributions of sensors and actuators, one system is designed. This system will have multiple actuators and sensors, which are not all used in every measurement. By switching connections, different sensor and actuator distributions can be tested without changing the physical properties of the beam. This means that any differences in measurement will be caused by the different sensor and actuator distributions, and not by measuring on a different system that might have sligthly different mechanical properties.

The system is designed in such a way that the actuators and sensors are placed at the optimal locations. These optimal locations are the modal strain peaks for every mode. At all of the locations (coordinates along the beam) where actuators are placed, sensors are placed at the opposite face of the beam. In this way, the sensors and actuators form collocated pairs.

To make a fair comparison of the damping performance, the number of actuators used

for controlling one mode is equal between all measurements. In all setups, 6 PiezoDrive BA3502 actuators are used for controlling one mode. This means that for controlling the first four vibration modes, 24 actuators are used.

Top view – Actuator side



Bottom view – Sensor side
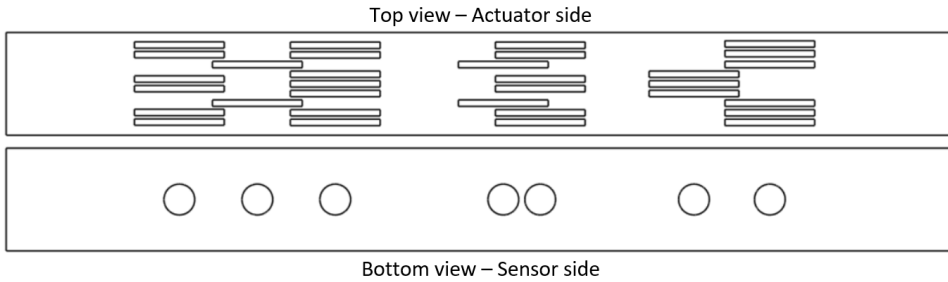
Figure 3.6: Schematic overview of actuator and sensor distribution

Three different layouts of sensors and actuators will be compared. Those setups are:

- **Setup a**: perfect-sensing and perfect-actuation.

  All of the 6 actuators are located at the same maximum modal strain location of the specific mode of interest. At the same beam coordinate, a dual and collocated sensor is placed at the opposite face of the flexure. The input signal for the 6 actuators is provided by one high voltage amplifier. Therefore, the 6 actuators at the same location behave like one large actuator. In this way, a perfect-actuated setup is created.

- **Setup b**: over-actuation and perfect-sensing.

  Here, the actuators are located at all modal strain peaks. The actuators intended to suppress mode 3 are distributed in 2 groups of 3. For mode 4, the actuators are distributed in 3 groups of 2. In this setup the actuators are located at all modal strain peaks, but only 1 active sensor is used per mode. So, in this setup, not all sensors and actuators are collocated. The goal of this setup is to show the benefits of over-actuation, while also showing the drawbacks of using over-actuation in combination with perfect-sensing.

- **Setup c**: over-actuation and over-sensing.

  In the third setup, over-actuation is combined with over-sensing. Both the actuators and the sensors are located at all modal strain peaks. In this way, all the actuators have a collocated sensor.

In figure 3.7, a picture of the cantilever beam in the lab can be seen. On the left side, the distribution of the actuators is shown. The sensor distribution can be seen in the right picture. The actuators and sensors are attached to the aluminum flexure with 'UHU Plus Endfest 300' epoxy. The whole setup is placed on an active vibration isolation table to suppress external noise and make sure measurements are repeatable. To introduce external vibrations into the beam. a piezoelectric stack is placed near the root of the beam. In order to measure vibrations at the tip of the beam, an accelerometer is attached.
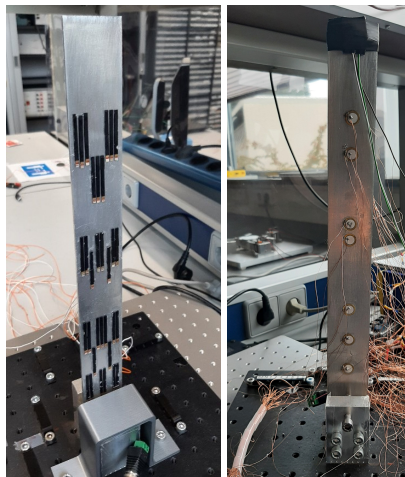
Figure 3.7: Pictures from setup in lab (a) Actuator side; (b) Sensor side

### 3.3.2. CONTROL ALGORITHM

Positive postion feedback (PPF) is the control algorithm that will be used in the experiments. PPF is a well-known linear control method for active vibration control. The sensor signal is positively fed back trough a second order filter. This is shown schematically in figure 3.8.
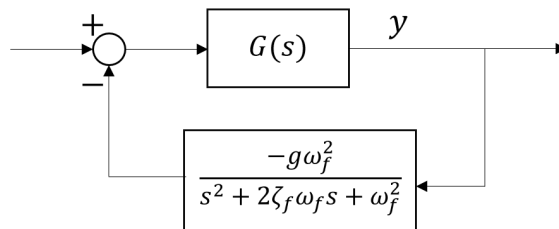


Figure 3.8: Block Diagram of PPF controller

The PPF controller is essentially a second order low-pass filter. The transfer function of the filter is given by equation 3.1. The three tuning parameters of this filter are $g$, $\zeta_f$ and $\omega_f$. $g$ is the gain of the second-order filter. $\zeta_f$ is the damping ratio of the low-pass filter, and $\omega_f$ is the filters corner frequency.

$$C(s) = \frac{-g\omega_f^2}{s^2 + 2\zeta_f\omega_f s + \omega_f^2} \tag{3.1}$$

To control the first four vibration modes, 4 controllers will be designed. The controllers are tuned using the guidlines based on maximum damping and $H_2$ optimization [21]. In the

experimental setup, the PPF controller is implemented in discrete form in LabVIEW. The LabVIEW program is running on a CompactRIO FPGA controller. The sampling frequency of the discrete controller is 10 kHz.

To make an equal comparison, the PPF controller is not changed between the different setups. So, the only difference is the distribution of the active actuators and the number of sensors used.

### 3.3.3. FREQUENCY RESPONSE MEASUREMENT

In the first experiment, the frequency response of the system is measured. To introduce vibrations into the system, the cantilever beam is excited at the root by the piezoelectric stack. The input of the stack is a sinusoidal voltage with a frequency varying from 1 to 2000 Hz.

First, the undamped system is identified by turning of the control algorithm. Then, the control algorithm is turned on and the system response is measured for the three different distributions of sensors and actuators. The measurement data will then be processed in Matlab, and the frequency response of the different systems will be compared.

### 3.3.4. TIME RESPONSE MEASUREMENT

Next to the analysis of the damping performance in frequency domain, there will also be a measurement of the time response of the different setups. To obtain relevant time-domain data, a step signal will be provided to the piezoelectric stack. When a step signal is provided to the stack, the flexure will be excited with an impulse-like force at the root. To analyse the time response of the different systems, the accelerometer signals of the different setups will be compared. From these signals, the settling time will be obtained and a comparison between the different setups can be made.

## 3.4. RESULTS AND DISCUSSION

In this section, the results of the two different measurements will be shown and the performance of the different actuator and sensor topologies will be evaluated. First, the frequency response measurement will be discussed in subsection 3.4.1. Then, the measurement of the time response of the different setups will be discussed in subsection 3.4.2.

### 3.4.1. FREQUENCY RESPONSE FUNCTION

Figure 3.9 shows the time data that is collected from a measurement on setup a.

In figure 3.9a, the signals going to the actuators are shown. The top plot shows the input signal going to the piezoelectric stack at the root of the flexure. As can be seen, the stack is actuated with a sinusoidal voltage with increasing frequency.

The bottom plot shows the output voltages of the PPF controllers. As explained in the method, setup a consists of 4 sensors, and actuators located at 4 different locations. These collocated sensor-actuator pairs all have an individual PPF control loop. The different PPF controllers are targeted to control different frequencies. This can also be observed in figure 3.9a, as the peak control force occurs at different times.

Figure 3.9b shows the outputs of the 7 piezoelectric sensors and the accelerometer. Here, it can be seen that at certain moments, the sensor output has a peak. This occurs

when the stack is actuated at a frequency close to the resonance frequencies of the system.



(a)

(b)
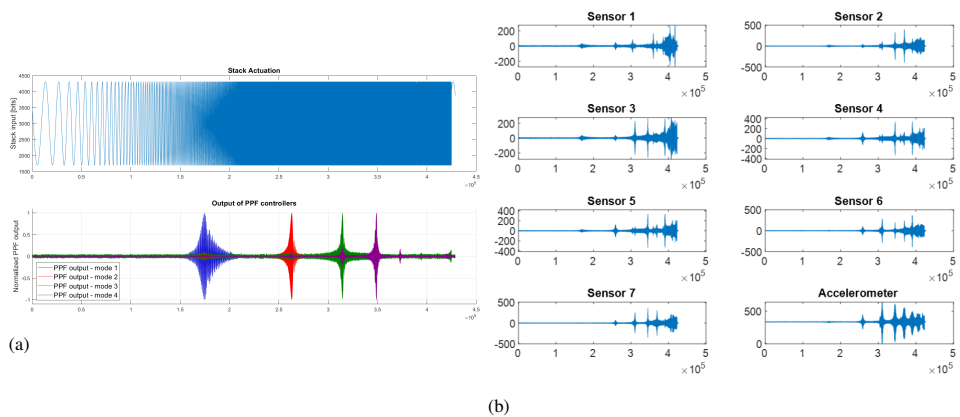
Figure 3.9: (a) Actuator signals; (b) Sensor signals

The data from figure 3.9 is processed in Matlab. With the 'tfestimate' function, the transfer functions can be estimated from the actuator and sensor data. In figure 3.10 the transfer function from the piezo stack actuator to the accelerometer is shown. So, this transfer function is relating a disturbance at the root of the flexure to the tip vibration.
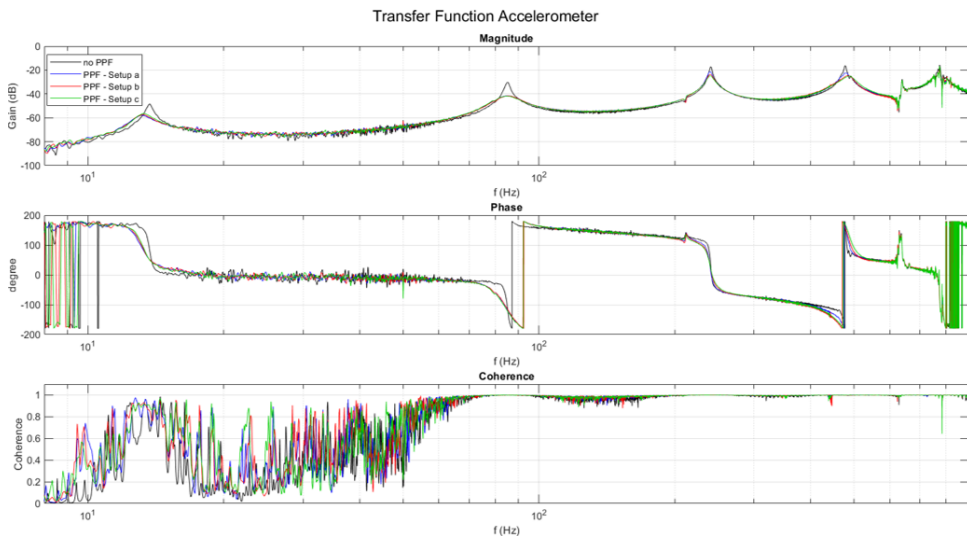


Figure 3.10: Transfer function from stack to accelerometer

The first two modes are configured in a perfect-sensing and perfect-actuation way for all three setups. Only the modes that have multiple modal strain peaks have a different distribution of sensors and actuators and therefore only the damping of mode 3 and 4 will be analysed in detail. In figures 3.11a and 3.11b, a zoomed-in view is shown for mode 3

and mode 4 respectively. The maximum values of the magnitude are reported in table 3.1.



(a)                                                     (b)
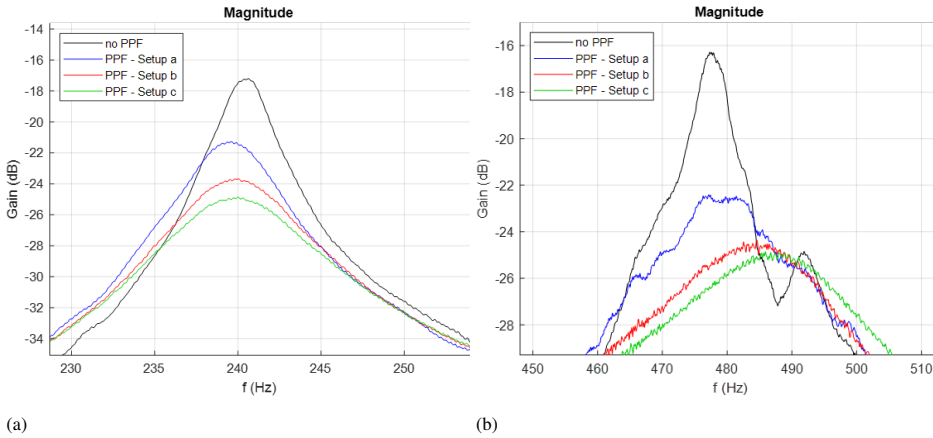
Figure 3.11: Transfer function from figure 3.10 - zoomed in at (a) Mode 3; (b) Mode 4

| Measurement | Mode 3 max value (dB) | Improvement compared to Setup a (dB) | % | Mode 4 max value (dB) | Improvement compared to Setup a (dB) | % |
|---|---|---|---|---|---|---|
| No PPF | -17.20 | — | — | -16.28 | — | — |
| PPF - Setup a | -21.31 | 0 | 0 | -22.46 | 0 | 0 |
| PPF - Setup b | -23.68 | 2.37 | 23.8 | -24.39 | 1.93 | 19.9 |
| PPF - Setup c | -24.97 | 3.65 | 34.3 | -25.08 | 2.62 | 26.0 |

Table 3.1: Maximum magnitude value in transfer function from figure 3.10 for mode 3 and mode 4

From table 3.1, it can be seen the reduction of the resonance peak of mode 3 is 4.11 dB for setup a, 6.48 dB for setup b and 7.77 dB for setup c. The performance relative to setup a is also shown in table 3.1. Here, it can be seen that the reduction of the resonance peak is 2.37 dB (23.8%) larger for setup b, and 3.65 dB (34.3%) larger for setup c.

For mode 4, it can be concluded that setup a suprresses the resonance peak by 6.18 dB. Setup b has a peak reduction of 8.11 dB and setup c reduces the resonance peak by 8.80 dB. So compared to the performance of setup a, setup b has a 1.93 dB (19.9%) larger peak suppression, and setup c even has a 2.62 dB (26.0%) better performance. From these values, it can be concluded that distributing the control actuators along the flexure increases the damping performance. However, using only over-acutation is still not optimal as not all of the actuators are using information about the local strain in the flexure. By combining over-actuation with over-sensing, all of the actuators can be used optimally and the damping performance is even better.

### 3.4.2. TIME RESPONSE

The time response of the different setups is shown in figure 3.12. At t = 0 s, the system is actuated with an impulse-like disturbance at the root of the flexure. For this experiment, the settling time is defined as the time it takes for the signal to reach and stay within the equilibrium state (within the dashed lines in figure 3.12).
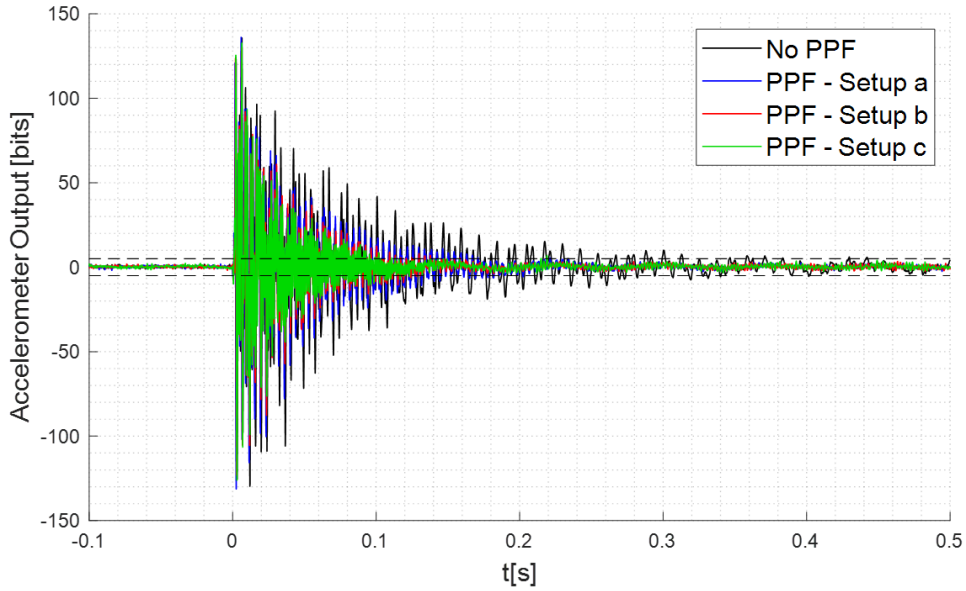


Figure 3.12: Time response: tip accelerometer signal

The settling times of the different setups are shown in table 3.2. Similarly to the frequency response experiment, it can be concluded that the damping performance of setup b is better than the performance of setup a. The settling time of setup b is 41 ms lower, which means an improvement of 25.2%. For the design with over-actuation and over-sensing (setup c), the damping performance is even better. Here, the settling time is 61 ms lower compared to setup a, which is an improvement of 37.4%.

| Measurement | Settling time (ms) | Improvement compared to Setup a (ms) | % |
|---|---|---|---|
| No PPF | 371 | — | — |
| PPF - Setup a | 163 | 0 | 0 |
| PPF - Setup b | 122 | 41 | 25.2 |
| PPF - Setup c | 102 | 61 | 37.4 |

Table 3.2: Comparison of settling times of different setups

## 3.5. CONCLUSION

In this paper, a new method for placing sensors and actuators for the implementation in AVC has been proposed. From state-of-the-art literature, it has been shown that the optimal location of sensors and actuators is at locations of maximum modal strain.

Experimental results show that using an over-actuated design leads to a better resonance peak reduction. However, when over-actuation is used in combination with perfect-sensing, there are still limitations on the damping system design because of the non-collocation of some actuators. This could be solved by implementing both over-actuation and over-sensing and thereby creating a fully collocated setup.

From experiments, it has been concluded that using an over-actuation and over-sensing strategy is beneficial for damping higher order modes of flexural elements. For modes 3 and 4, the reduction in resonance is respectively 34.3% and 26.0% better compared to the state-of-the-art damping methods. In time domain, the new strategy reduces the settling time by 37.4%.

If this new strategy of distributing the actuators and sensors would be implemented in industrial machines, it would mean that the speed and precision at which these machines operate can improve. Therefore, this development could be a new step into the direction of following Moore's law.

## REFERENCES

[1] Moore, G. E. (1965). Cramming more components onto integrated circuits.

[2] Larry L Howell, Spencer P Magleby, Brian Mark Olsen, and John Wiley. *Handbook of compliant mechanisms*. Wiley Online Library, 2013.

[3] A. Preumont. *Vibration Control of Active Structures: An Introduction.* Solid Mechanics and Its Applications. Springer, 2013. ISBN 9789400720336.

[4] Jan Lunze. *Feedback control of large scale systems*. Prentice Hall PTR, 1992.

[5] Vahab Nekoukar and Abbas Erfanian. A decentralized modular control framework for robust control of fes-activated walker-assisted paraplegic walking using terminal sliding mode and fuzzy logic control. *IEEE transactions on biomedical engineering,* 59(10):2818–2827, 2012.

[6] Bruant, I., & Proslier, L. (2015). Improved active control of a functionally graded material beam with piezoelectric patches. *Journal of Vibration and Control*, 21(10), 2059-2080.

[7] Daraji, A. H., Hale, J. M., & Ye, J. (2018). New methodology for optimal placement of piezoelectric sensor/actuator pairs for active vibration control of flexible structures. *Journal of Vibration and Acoustics*, 140(1).

[8] Zorić, N. D., Simonović, A. M., Mitrović, Z. S., & Stupar, S. N. (2013). Optimal vibration control of smart composite beams with optimal size and location of piezoelectric sensing and actuation. *Journal of Intelligent Material Systems and Structures*, 24(4), 499-526.

[9] Lu, E., Li, W., Yang, X., Wang, Y., & Liu, Y. (2018). Optimal placement and active vibration control for piezoelectric smart flexible manipulators using modal $H_2$ norm. *Journal of Intelligent Material Systems and Structures*, 29(11), 2333-2343.

[10] K Ramesh Kumar and S Narayanan. Active vibration control of beams with optimal placement of piezoelectric sensor/actuator pairs. *Smart Materials and Structures,* 17 (5):055008, 2008.

[11] Lee, C. K., & Moon, F. C. (1990). Modal sensors/actuators.

[12] Preumont, A., François, A., De Man, P., & Piefort, V. (2003). Spatial filters in structural control. *Journal of sound and vibration*, 265(1), 61-79.

[13] Sumali, H., Meissner, K., & Cudney, H. H. (2001). A piezoelectric array for sensing vibration modal coordinates. *Sensors and Actuators A: Physical,* 93(2), 123-131.

[14] M. Schneiders MJG van de Molengraft and M. Steinbuch, "*Benefits of overactuation in motion systems,"* tech. rep., 2004.

[15] N. Tanaka and S. D. Snyder, "Cluster control of a distributed-parameter planar structure—Middle authority control," *The Journal of the Acoustical Society of America,* vol. 112, pp. 2798–2807, 12 2002.

[16] Vivek Gupta, Manu Sharma, and Nagesh Thakur. Optimization criteria for optimal placement of piezoelectric sensors and actuators on a smart structure: a technical review. *Journal of Intelligent Material Systems and Structures*, 21(12):1227–1243, 2010.

[17] Li Bin, Li Yugang, Yin Xuegang, and Huang Shanglian. Maximal modal force rule for optimal placement of point piezoelectric actuators for plates. *Journal of Intelligent Material Systems and Structures,* 11(7):512–515, 2000.

[18] José M Simoes Moita, Victor M Franco Correia, Pedro G Martins, Cristovao M Mota Soares, and Carlos A Mota Soares. Optimal design in vibration control of adaptive structures using a simulated annealing algorithm. *Composite Structures,* 75(1-4):79– 87, 2006.

[19] Tae-Woo Kim and Ji-Hwan Kim. Optimal distribution of an active layer for transient vibration control of a flexible plate. *Smart Materials and Structures*, 14(5):904, 2005.

[20] Zhi-cheng Qiu, Xian-min Zhang, Hong-xin Wu, and Hong-hua Zhang. Optimal placement and active vibration control for piezoelectric smart flexible cantilever plate. *Journal of Sound and Vibration,* 301(3-5):521–543, 2007.

[21] Paknejad, A., Zhao, G., Osée, M., Deraemaeker, A., Robert, F., & Collette, C. (2020). A novel design of positive position feedback controller based on maximum damping and $H_2$ optimization. *Journal of Vibration and Control*, 26(15-16), 1155-1164.

# 4

# CONCLUSION

In this thesis, a new topology of sensors and actuators has been proposed to improve the damping performance of flexible system. This was motivated by the ever-increasing demands for high-precision machines. These machines use flexures in the positioning systems. The structural resonance modes are limiting the maximum bandwidth of these machines. So, to obtain the highest possible bandwidth, the vibration modes in these flexures should be damped as much as possible.

After a literature survey, it was concluded that the optimal location of sensors and actuators in active vibration control is at locations of maximum modal strain. Another finding from the literature survety was that in the state-of-the-art active damping methods, underactuation and perfect-actuation are the commonly used methods. However, over-actuation has shown to be better in terms of modal controllability and disturbance rejection [1].

Although it has been proven that over-actuation is better in terms of modal controllability, there are no studies present were over-actuation is used in active vibration control.

In this thesis, over-actuation in combination with over-sensing is implemented in active vibration control. In an experimental setup, the damping performance of this setup was compared with 2 other setups. The first setup uses perfect-actuation and perfect-sensing and the second setup uses over-actuation and perfect-sensing.

The experimental results showed that using an over-actuation and over-sensing strategy is beneficial for damping higher order modes of flexural elements. For the third mode, the maximum maginitude in the frequency response function was reduced by 34.3%, and for the fourth mode the maximum magnitude was reduced by 26.0% compared to the state-of-the-art damping method. In time domain, the settling time was reduced by 37.4% compared to the perfect-actuation and perfect-sensing setup.

So, in this thesis it has been shown that the damping performance in active vibration control can be improved by distributing the sensors and actuators along the host structure. If this method would be implemented in industrial machines, the bandwidth of these machines can be higher. This would mean that the speed and precision at which these machines operate can improve. Therefore, this development could be a new step into the direction of following Moore's law.

All in all, the experimental setup was designed in a structured way with the acutators and sensors placed at their optimal location. Then, this setup was created in a real-life setup in the lab, and the damping performance was tested and compared with the damping performance of systems with other sensor-actuator distributions. So, it can be concluded that all of the research objectives that were stated in section 1.4 have been fulfilled succesfully.

### FUTURE STEPS

In this research field, a lot of steps could still be taken. This thesis was the first study to implement over-actuation and over-sensing in active vibration control. However, experiments were only performed on a simple 'one-dimensional' cantilever beam, where only bending modes were considered. In a future work, the same strategy of distributed over-actuation and over-sensing could be applied on flexible plates, where both bending modes and torsional modes are important.

Another direction of research could be into modal filters. In this study, the control system was decentralized as it has benefits in terms of simplicity and computational efforts. However, using (discrete) modal filters that combine data of different sensors by a smart algorithm could even improve the observability of the modes of interest. If modal filters are used for both actuation and sensing, it should theoretically be possible to perfectly sense and actuate the desired modes without any spillover to/from other modes. If this would be implemented in the right way (so for example the distance between different sensors/actuators should not be too large), the damping performance could even be better. So, a next study could focus on how to optimally implement modal fitering in active vibration control.

A third direction that might be an interesting step is more on the practical side. As the number of actuators and sensors increase, the number of required wires also increases. This will quickly create a chaotic experimental setup. For proving the theory of over-actuation and over-sensing in AVC, this is not a huge problem. However, when this method is to be applied in a real-life physical machine, having a mess of wires is not an option. So, a future study could focus on how to make the practical implementation in a way that it is easy to implement and has a reliable performance. For example, this could be done by creating a flexible PCB that is attached onto the flexure. Another option is to embed the wiring into the flexure in the manufacturing process. In theory, not only the wires but also the actuators and sensors could be embedded in the flexure during the manufacturing process. All things considered, the practical implementation of systems with a lot of actuators and sensors is a very important topic.

### REFERENCES

[1]  M. Schneiders MJG van de Molengraft and M. Steinbuch, "*Benefits of overactuation in motion systems,*" tech. rep., 2004.

# A

## EXPERIMENTAL SETUP

In this appendix section, the experimental setup will be explained in detail. First, the different actuator and sensor topologies will be explained and visualized. Then, the whole setup including all of the components will be described. Also, a schematic wiring diagram will be shown and the color coding of the enameled wires in the experimental setup will be explained.

# A

# Details of the three different experimental setups

The placement of the sensors and actuators is based on the modal strain distribution. Three different setups will be made. These setups are:

- Setup a: Perfect sensing and perfect actuation
- Setup b: Perfect sensing and over-actuation
- Setup c: Over-sensing and over-actuation

In all three setups, the number of actuators and the control algorithm are exactly the same. Therefore, the damping performance of the system only depends on the topology of sensors and actuators. So in this way, the most fair comparison can be made between the different setups. The modal strain distribution of the first 4 bending modes of a cantilver beam is shown in the figure below.
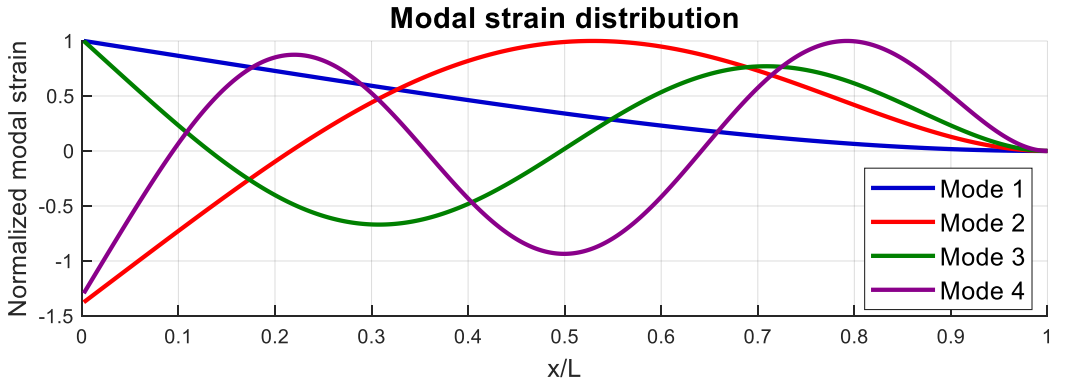


**Setup a:** Perfect sensing and perfect actuation

In this setup, the actuators and sensors are both placed at one modal strain peak per mode. So, the blue actuators and sensor are used for mode 1. As can be seen from the modal strain distribution plot, these actuator are placed at the maximum modal strain location for mode 1 (because of the clamping mechanism the actuators could not be located closer to the root). The colors in this schematic figure correspond with the colors in the plot. So, red is used for mode 2, green for mode 3 and purple for mode 4. This sensor/actuator distribution is the most commonly used in state-of-the-art literature and it will serve as a setup for comparison of damping performance.



**Top view – Actuator side**

**Bottom view – Sensor side**
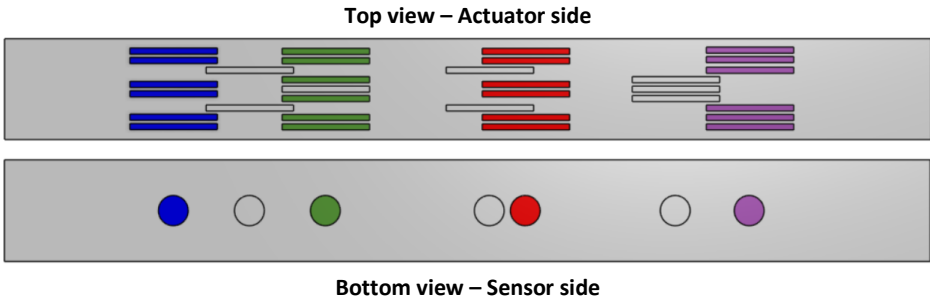
## Setup b: Perfect sensing and over-actuation

In this setup, actuators are located at all modal strain peaks for every mode. This means that mode 2 has 2 groups of 3 actuators at both of the modal strain peaks. Mode 4 has 3 groups of 2 actuators, which are located at each of the three modal strain maxima. For the sensor side, the setup is similar to setup a. Therefore, not all actuators have a collocated sensor.

**Top view – Actuator side**



**Bottom view – Sensor side**
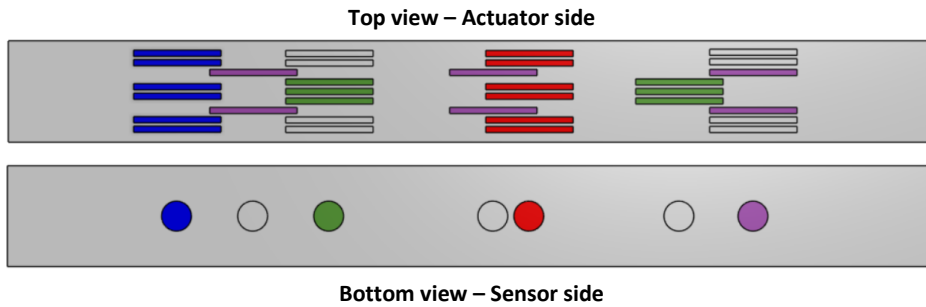
## Setup c: Over-sensing and over-actuation

In this setup, both actuators and sensors are located at all modal strain peaks for every mode. This means that the system is fully collocated. This is the new proposed design, and it is expected that the damping performance of setup c is better than setup b and a.

**Top view – Actuator side**



**Bottom view – Sensor side**

**A**
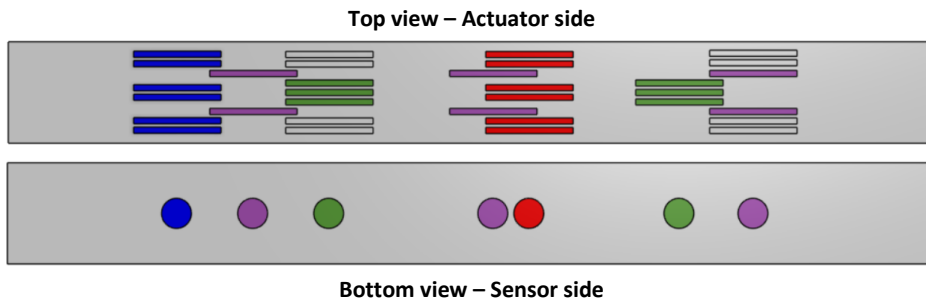
# Experimental setup

In the following table, all of the components of the experimental setup are described. Also, the most important function of these components are mentioned.

| Component | Type/Details/Dimension | Function |
|---|---|---|
| Flexure | Aluminum 370x40x2 mm | Flexure that is used in the experiments |
| Clamping mechanism | Manufactured out of aluminum | Clamping the flexure at the root. This creates a cantilever beam. Also, a pre-tensioning bolt for the piezo stack is included in the clamp |
| Vibration Isolation Table | Table-Stable TS-150 | Isolate external vibrations for repeatable measurements and lowering external noise |
| Piezo Bender Actuator | PiezoDrive BA3502 | Piezo Actuators for vibration control |
| Piezo Stack Actuator | *Model name unkown* | The piezo stack at the root of the beam introduces external vibrations into the system |
| High Voltage Amplifier | PiezoDrive BD300 | Voltage amplifier for the PiezoDrive BA3502 actuators |
| High Voltage Amplifier | PiezoMechanik LE 150/200 | Voltage amplifier for the Piezo Stack |
| Piezo Sensor | Murata 7bb-12-9 | Measuring the local strain in the flexure |
| Accelerometer | Sparkfun ADXL337 | Measure acceleration at the tip of the flexure |
| Controller | NI CompactRIO | Obtain data from sensors, calculate control voltage by using a control algorithm, apply control voltage and log data. |
| Analog Input Module | NI9201 | Used for obtaining data from the sensors. Wires from the sensors are connected to the NI9201 module. This module is placed in the CompactRIO chassis. |
| Analog Output Module | NI9264 | Used for outputting disturbance and control voltages. Wires from the NI9264 module are connected to the respective amplifiers for the actuators. This module is placed in the CompactRIO chassis. |
| Wires | Enameled copper wire Diameter = 0.20 mm | Enameled wires are used because the weight of these wires is very low and therefore the influence on the system is minimized. Also, enameled wires are relatively easy for soldering |
| Lab Power Supply | 24V – max 5 A power supply | For powering the BD300 Amplifiers |

On the next page, a figure of the experimental setup is shown. Here, most of the components are indicated in the figure. Also, two separate pictures of the actuators and the sensors on the aluminum flexure are shown.

Accelerometer

PiezoDrive BD300 amplifiers with 3D printed case

PiezoMechanik High Voltage Amplifier

Aluminum Flexure

Piezo Stack

Clamping Mechanism

Vibration Isolation Table

CompactRIO with NI9201 and NI9264 modules
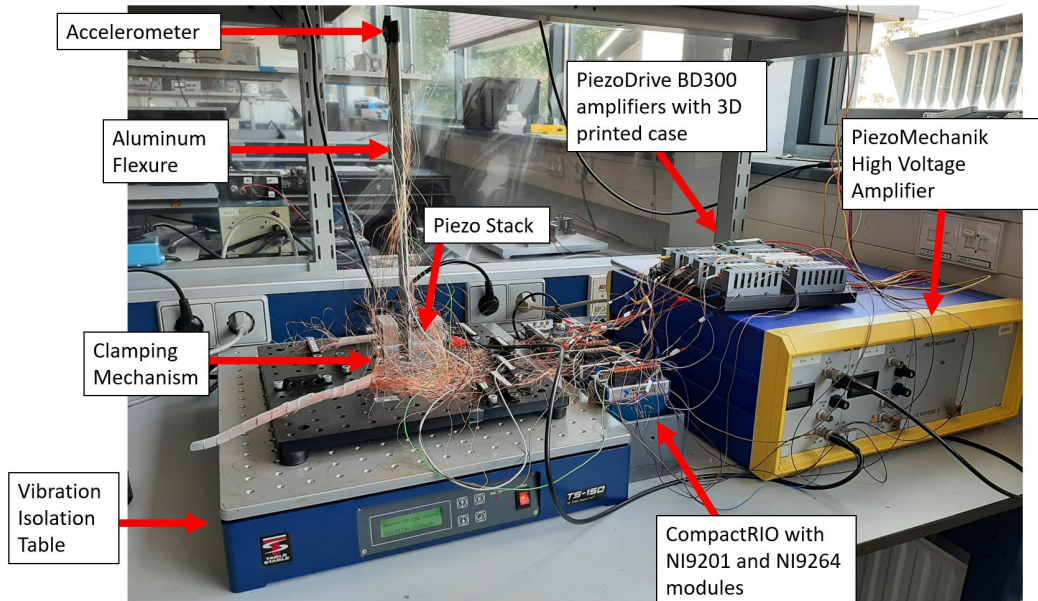
## BA3502 Piezo Bender Actuators
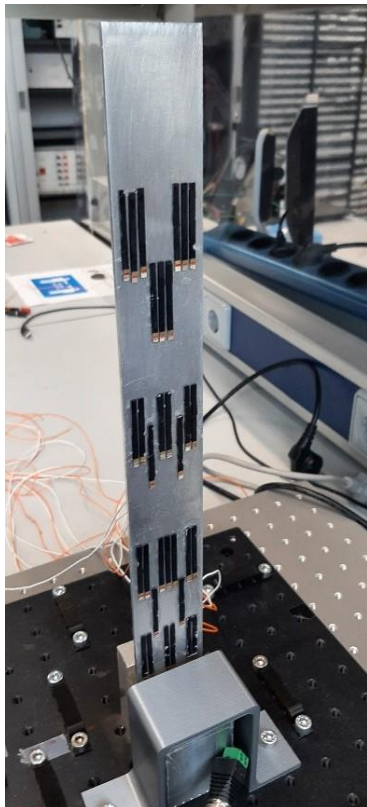


## Piezo Sensors
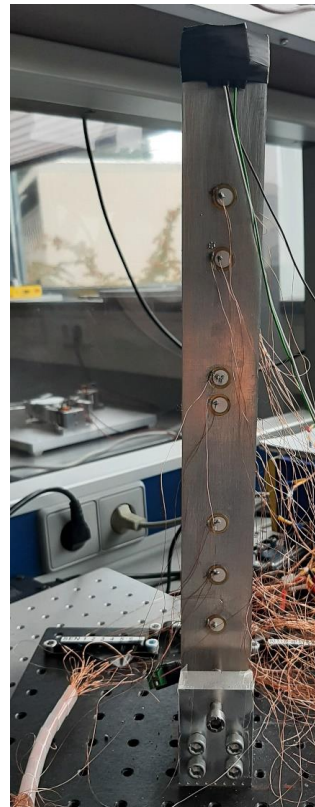
# Color coding of wires

As can be seen in the figures from the experimental setup, all of the wires to the piezo actuators and sensors are enameled wires (and all have the same color). So, for practical purposes a color coding labling system is made. The most important function of this labling system is to make sure that the user of the setup understands which wire is connected to which actuator. So, when one wants to change the setup and use another actuator layout, it is important to know which wires to change.

All of the actuators that are used as one group in all of the setups (so for example the 6 actuators for mode 1 are used in all setups) are grouped, and a name is given to the actuator group. Next to the name, a color is given to the group. In the experimental setup, the colors are applied by electrical tape in various colours.

The naming system is as follows: The first number is the intended mode for the actuators. The second number is the location along the beam (so a 2 means the second actuator group for that mode, starting from the root of the flexure). The last number indicates the number of actuators in the group.
To make it clear, actuator 4.3.2 indicates that the actuator group is used to dampen mode 4. The group is the third group for mode 4 in this setup, and 2 actuators are used. In the following pages, all of the actuator groups are shown with the name and color code.

## Mode 1

## Actuator 1



Color code wires:          +  [red]                    GND [red/white]

## Mode 2

## Actuator 2



Color code wires:          +  [blue]                    GND [blue/white]
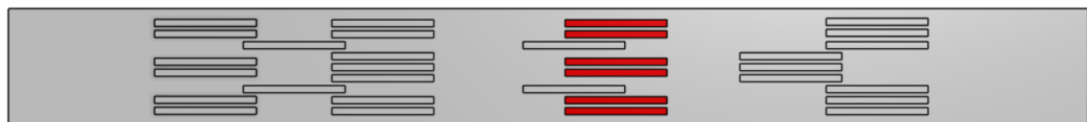
# Mode 3

## Actuator 3.1.4

Color code wires:  +  GND

## Actuator 3.1.2

Color code wires:  +  GND

## Actuator 3.1.1

Color code wires:  +  GND

## Actuator 3.2.3
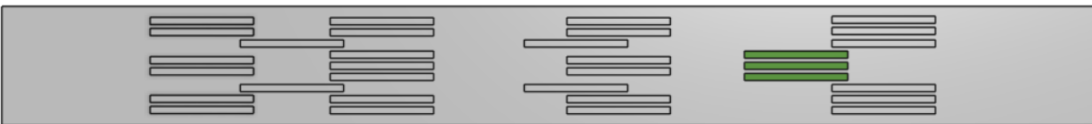
Color code wires:  +  GND

**A**

## Mode 4

### Actuator 4.1.2



Color code wires:          **+**  [black/red]              **GND** [black/red/white]

### Actuator 4.2.2



Color code wires:          **+**  [black/blue]              **GND** [black/blue/white]
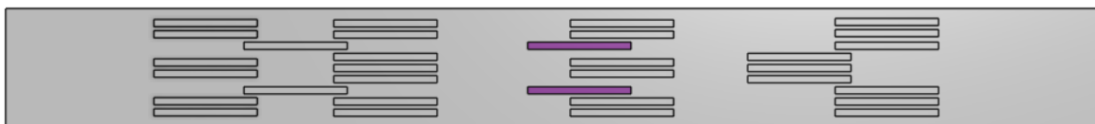
### Actuator 4.3.4



Color code wires:          **+**  [black]              **GND** [black/white]
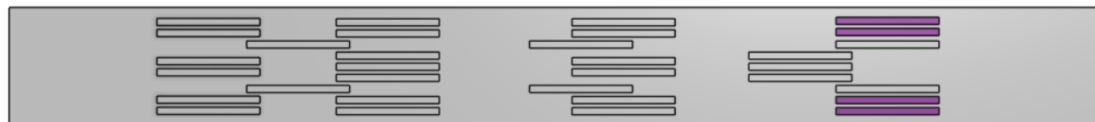
### Actuator 4.3.2



Color code wires:          **+**  [black/yellow]              **GND** [black/yellow/white]
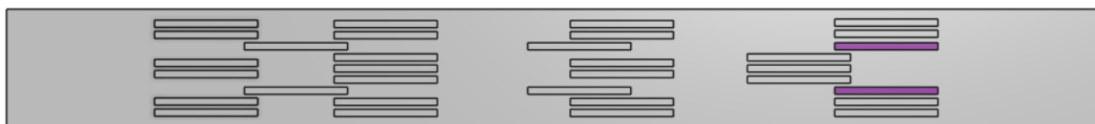
# Which wires to connect to create different setups

## Perfect-actuation



To create the perfect-actuated setup, the following actuator groups need to be connected to the amplifiers.

| Amplifier | Actuator groups |
| --- | --- |
| 1 (mode 1) | Actuator 1 |
| 2 (mode 4) | -    Not used in this setup |
| 3 (mode 3) | Actuator 3.1.4 and Actuator 3.1.2 |
| 4 (mode 4) | -    Not used in this setup |
| 5 (mode 2) | Actuator 2 |
| 6 (mode 3) | -    Not used in this setup |
| 7 (mode 4) | Actuator 4.3.4 and Actuator 4.3.2 |

## Over-actuation
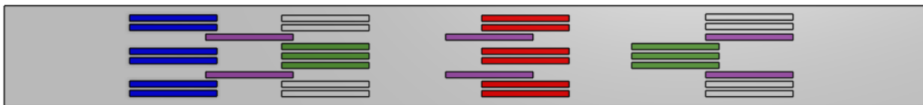


For the over-actuated setup, the following connections should be applied.

| Amplifier | Actuator groups |
| --- | --- |
| 1 (mode 1) | Actuator 1 |
| 2 (mode 4) | Actuator 4.1.2 |
| 3 (mode 3) | Actuator 3.1.1 and Actuator 3.1.2 |
| 4 (mode 4) | Actuator 4.2.2 |
| 5 (mode 2) | Actuator 2 |
| 6 (mode 3) | Actuator 4.2.3 |
| 7 (mode 4) | Actuator 4.3.2 |

A
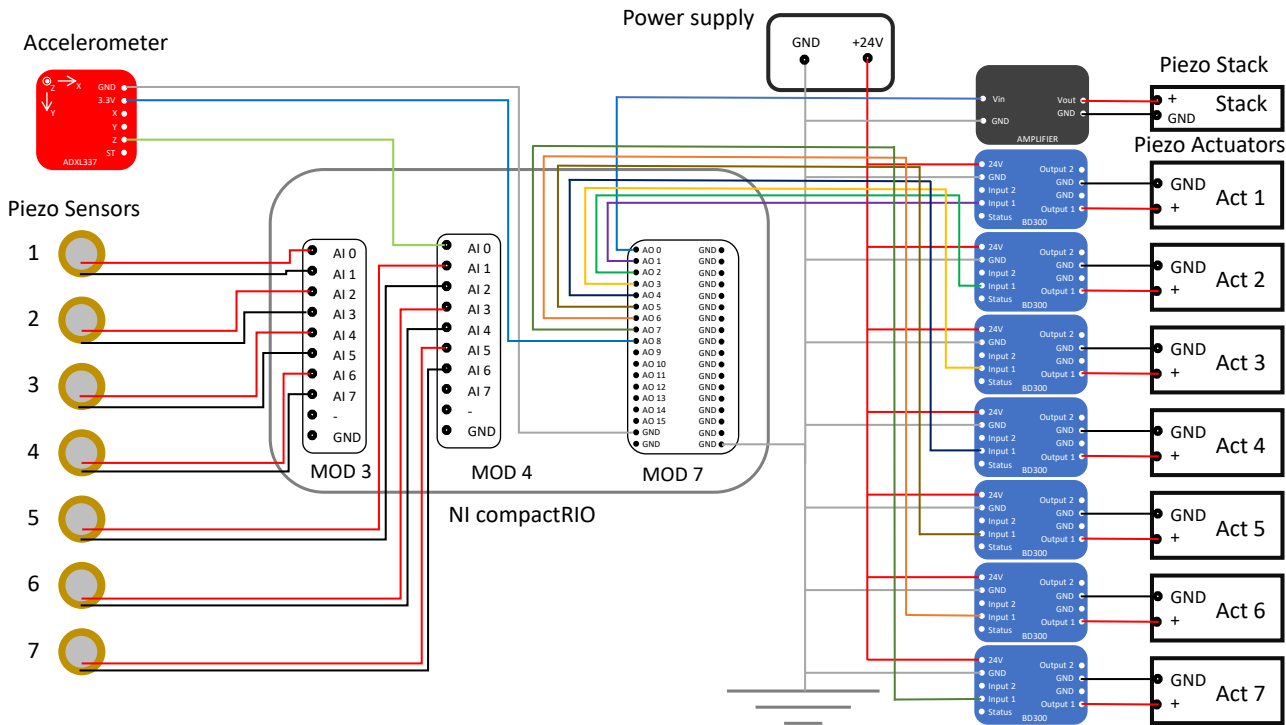
# B

# LABVIEW PROJECT EXPLANATION

In this appendix chapter, a step-by-step instruction will be given on how to use the Lab-VIEW file and how to obtain measurement data. Finally, it is explained how to make transfer functions from the measurement data file using Matlab.

**B**

**How to use the LabVIEW project file – Detailed description of important aspects**

In the following picture, the LabVIEW project file is shown. The LabVIEW project is used to implement control in the system and save the measurement data.  As can be seen below, the controller unit that is used is the NI-cRIO-9039-01C9917A. In module 3 and 4, the analog input module NI9201 is used to obtain the sensor voltages. In module 7, analog output module NI9264 is used to send signals to the amplifiers for the actuators.
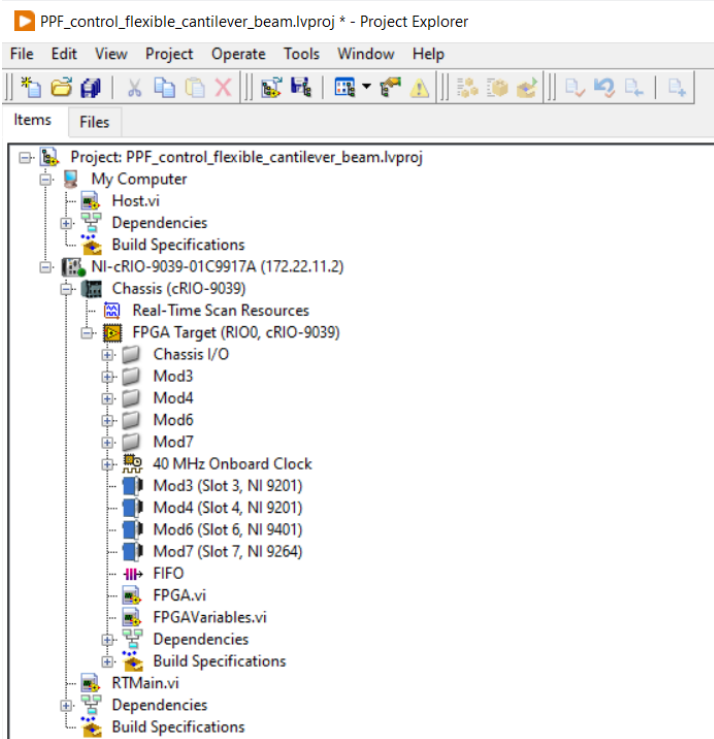


The most important files are Host.vi, RTMain.vi and FPGA.vi. The FPGA file is the file that includes the control algorithm. This is running on the compactRIO FPGA (Field Programmable Gate Array). If one wants to make adjustments to the FPGA.vi file, it needs to be recompiled. This compilation usually takes about 30 minutes to 1 hour. The file 'RTMain.vi' is used as an interface between the laptop and compactRIO, in this file, values can be changed (if a variable is made in the FPGA.vi file). Changes in RTMain only take a few seconds to adjust. So, variables that will be changed a lot (for example controller parameters) should ideally be put in the RTMain.vi file. Finally, the Host.vi is running on the laptop. This file collects all of the data and saves it on the hard disk of the laptop. This data can later be used in Matlab or other programs for analysis. In the next figure, the function of the three most important files is shown schematically.
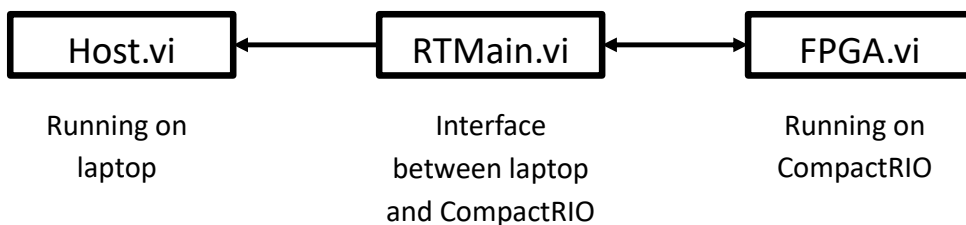
**FPGA.vi**

In the FPGA.vi file, the sensor data is collected. The sensor data is obtained from module 3 and 4 (the analog input modules NI9201). The piezoelectric sensors have 2 wires. The difference between the voltages of the two wires is taken as the output voltage from the sensor. This is done to avoid ground loops. For piezo sensor 7, a noisy signal was obtained. This might be caused by an incorrectly functioning port (Mod4/AI5). For this reason, the variable 'Strain Piezo 7b' is introduced. This solved the issue. So, in all of the files 'Strain Piezo 7b' is used instead of 'Strain Piezo 7'. In the figure below, it can be seen how the sensor data is obtained in the FPGA.vi file.
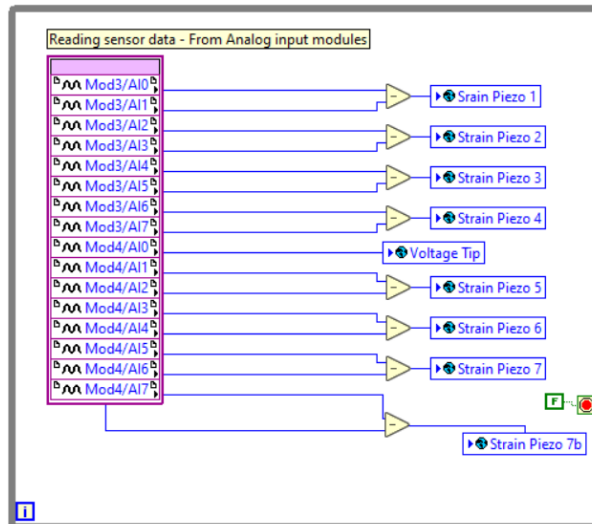


The FPGA.vi also generates the desired disturbance. For identification purposes, the system will be actuated with a sine disturbance. The sine is introduced in the FPGA.vi file. The frequency, amplitude and offset can all be changed in the RTMain.vi file. Also, the accelerometer needs to be provided a 3.3V supply voltage. This is implemented in the FPGA.vi file, as this does not need to be changed for different experiments.

The NI9264 analog output module is 16 bit +-10V (so 2 sided). This means that 10V corresponds to $\frac{2^{16}}{2} = 32768$. Therefore, 3.3V corresponds with a bit-value of: $\frac{3.3}{10} * \frac{2^{16}}{2} = 10922$. This is shown in the figure below.
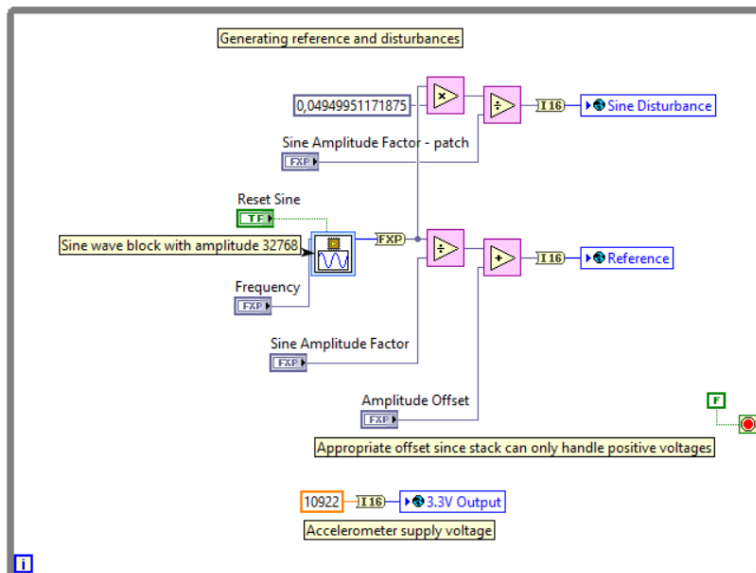
The FPGA file contains the control structure that is used. In the figure below, the control structure for the first collocated sensor-actuator pair is shown. First, data from the sensor 'Strain Piezo 1' is converted to fixed point representation. This is necessary for quick operation of the FPGA. Then, the value from the sensor is multiplied by the transfer function of the controller (the PPF filter). After this, the signal is multiplied by a gain, and then converted back from a fixed point to a floating point number. When the Boolean PPF 1 on is false, it means that the PPF controller is not used and all of the described steps are not performed, and instead a zero-value will be used.

If the Boolean value 'Add Disturbance 1', the sine disturbance will be applied to actuator 1. In this way, the system can not only be actuated by the stack, but also by all of the piezo patch actuators. The PPF signal and Disturbance signal are then added. A saturation block prevents actuator saturation, so voltages above the maximum limit will not be provided to the actuators. Finally, an offset is added to the signal (this is needed because of the working principle of the BD300 Amplifiers). The final signal will be saved in the FPGA variable 'Voltage Output Piezo 1' and will be sent to the analog output module. This loop iterates at a frequency of 10 kHz. For all other actuator/sensor pairs, the control structure is similar. The only difference between the different modes is the values in the transfer function block.
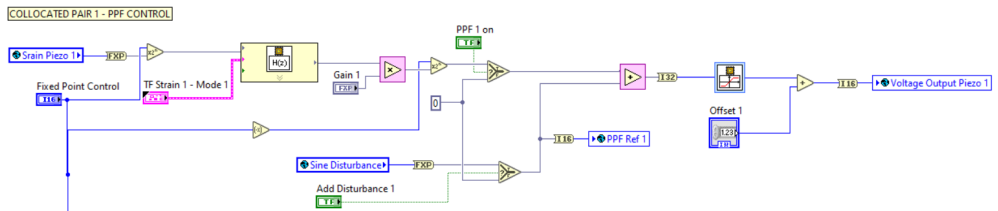


In the figure below, it is shown how a step signal is made. When the Boolean 'Step 2' is true, the signal will be equal to the number 'Step value 2'. Otherwise, the value will be 0. So, when the Boolean button is selected, a step signal will be sent to 'Voltage Output Disturbance'. Again, a saturation block is used to prevent actuator saturation.
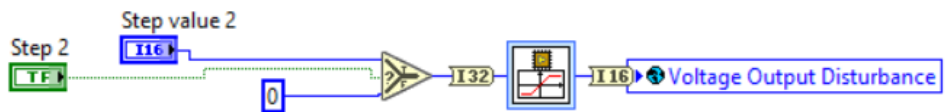
At the end of the FPGA file, all FPGA variables are written to FIFO. FIFO (First In First Out) is a data storage method. Data that is saved in FIFO can be opened in the RTmain.vi and Host.vi. Also, the output voltages are written to the output module in the FPGA file. This can be seen at the top of the figure.

**B**
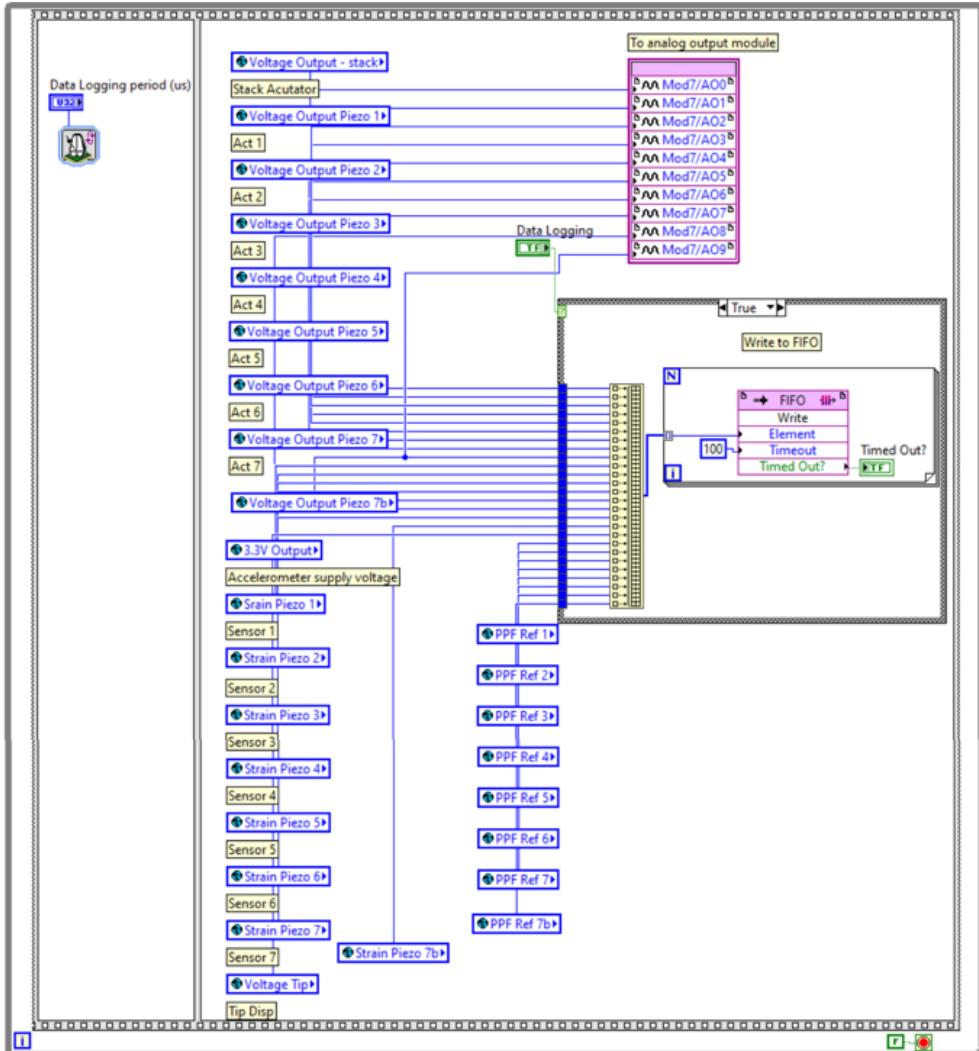
**RTMain.vi**

In the figure on the next page, the Front Panel of the RTMain.vi file is shown. In this panel, actuators can be quickly turned on and off. Also, a disturbance can be generated, the system can be switched between over-sensing or perfect-sensing mode, the data can be logged, and a step can be generated.

The following parameters can be seen in the RTMain.vi Front Panel. This list includes a small explanation for the user on what to select to perform certain actions.

- **Starting Freq:** Starting frequency of the chirp (sinusoid with increasing frequency) signal
- **Increase fraction:** Each step, the current frequency is multiplied by the increase fraction
- **Max Freq:** Maximum frequency of the chirp disturbance signal.
- **Increase:** Turn on to increase the current frequency (to start the chirp signal)
- **Data logging:** Turn on to log data to Host.vi file
- **Stop:** Press this button if you want to stop the RTMain.vi file
- **Amplitude Offset:** Offset of output signal to piezo stack
- **Offset 1-7:** Offset of output signal to actuator 1-7
- **Reset Sine:** Turn on to reset the sine disturbance (so if this is selected, disturbance is 0)
- **Over-Sensing On:** Turn on to use over-sensing. Turn-off to use perfect sensing
- **PPF 1-7 On:** Turn on to turn on the PPF control for actuator 1-7
- **Add Disturbance 1-7:** Turn on to add the chirp disturbance through actuator 1-7
- **Add Disturbance through stack:** Turn on to add chirp disturbance through stack
- **Sine Amplitude Factor – patch:** The chirp signal to the piezo patch actuators will be divided by the amplitude factor. So, a higher amplitude factor results in a lower voltage.
- **Sine Amplitude Factor:** The chirp signal to the piezo stack actuator will be divided by the amplitude factor. So, a higher amplitude factor results in a lower voltage.
- **Step Value:** Value of the step. This is provided to the piezo stack.
- **Offset Stack:** Offset of the step function for the stack.
- **Step on:** Turn on to apply step to piezo stack

At the beginning of the measurement, the user must make sure that both the Host.vi file and the RTMain.vi file are running (click the white arrow on the top left of the front panel). If everything is set up correctly, the indicator 'Timed Out?' on the RTMain.vi front panel should not blink, and in the block 'Current Freq', the current frequency of the disturbance signal should be displayed.

**B**
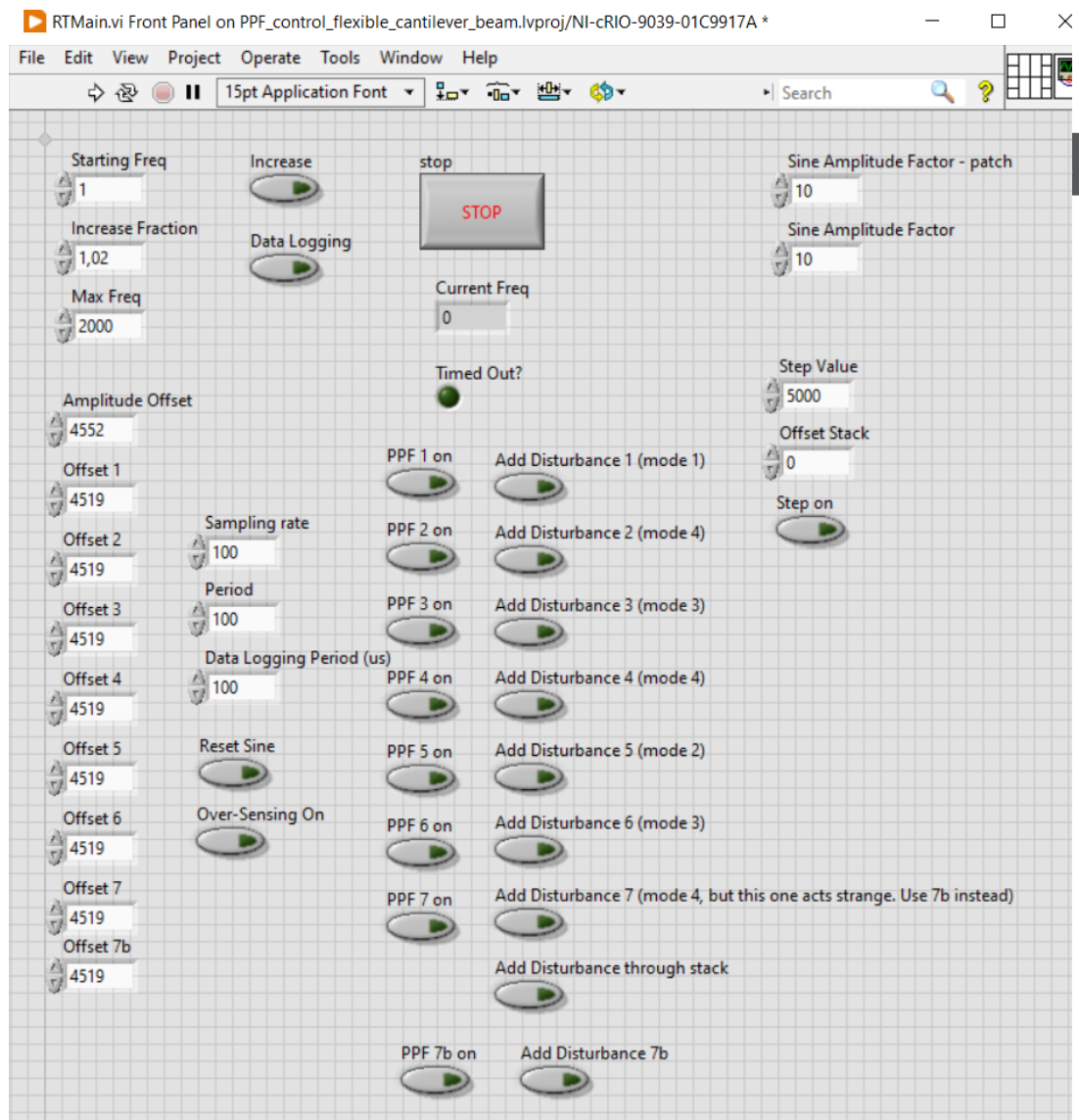
**Transfer function of PPF Controllers in LabVIEW**

In the RTMain.vi block diagram, the transfer functions of the different PPF controllers are defined. Controllers in LabVIEW are in discrete form. To obtain a discrete controller, the user can use Matlab to transform a continuous transfer function to a discrete transfer function.

**Pay attention!** The order of transfer function coefficients in LabVIEW is exactly opposite to the order in Matlab. So for example, denominator of the transfer function $\frac{1}{2s^2+3s+1}$ would be described in Matlab as [2 3 1]. In LabVIEW this is written as [1 3 2]. To avoid confusion, it is handy to use the fliplr command in LabVIEW. If this command is used, the same layout as Matlab (and most other programs you are probably used to).

To convert a transfer function from continuous form to discrete form, the 'Tustin' method is used in Matlab. The Matlab code for the PPF design for mode 1 is shown below.

```
%% PPF design for mode 1
f_sample = 10000;    %sampling frequency
zeta = 0.25;         %damping ratio of PPF filter
w_c = 14.07*2*pi;    %filter corner frequency (in rad/s)
k = 0.5;             %gain of PPF filter

Numerator = [-k*w_c^2];
Denominator = [1 2*zeta*w_c w_c^2];

H = tf(Numerator,Denominator);            %continuous
transfer function
H_discrete = c2d(H, 1/f_sample, 'Tustin');  %convert
continuous transfer function to discrete

numerator_mode1 = H_discrete.Numerator{1,1}    %discrete
numerator coefficients
denominator_mode1 = H_discrete.Denominator{1,1} %discrete
denominator coefficients
```

If this code is executed, the result is:

numeratormode1 = 1.0e-04 * [ -0.097474428673670  -0.194948857347340  -0.097474428673670]

denominatormode1 =  [1.000000000000000  -1.995511633208028   0.995589612750967]

These values are then inserted in LabVIEW in the following way. It can be seen that the numerator is a factor [1 2 1], so 1.0e-04 * [ -0.097474428673670  -0.194948857347340  -0.097474428673670] is simplified to -0.194948857347340e-04 * [ 1 2 1]

**Host.vi**

The third important file in the LabVIEW project is the Host.vi file. This file is entirely running on the laptop of the user, and is used to log measurement data.

In the front panel of the Host.vi file, a lot of waveform chart blocks can be seen. When the system is running, white lines will appear in the black areas. These white lines represent values (could be sensor data, actuator data, etc.)

In the block diagram of the Host.vi file, the data from the FIFO is read. The FIFO data is data that is obtained from the FPGA file. This data will be clustered into an array and is saved to a Measurement file. This can be seen in the picture below.

In the 'Write To Measurement File' block, some characteristics of the measurement file can be specified. For example, the filename and folder. Also, the format can be specified here. After trying multiple options, I found that using the LVM file extension, the data processing in Matlab will be the quickest.

In the figure below, the settings in the 'Write To Measurement File' are shown.
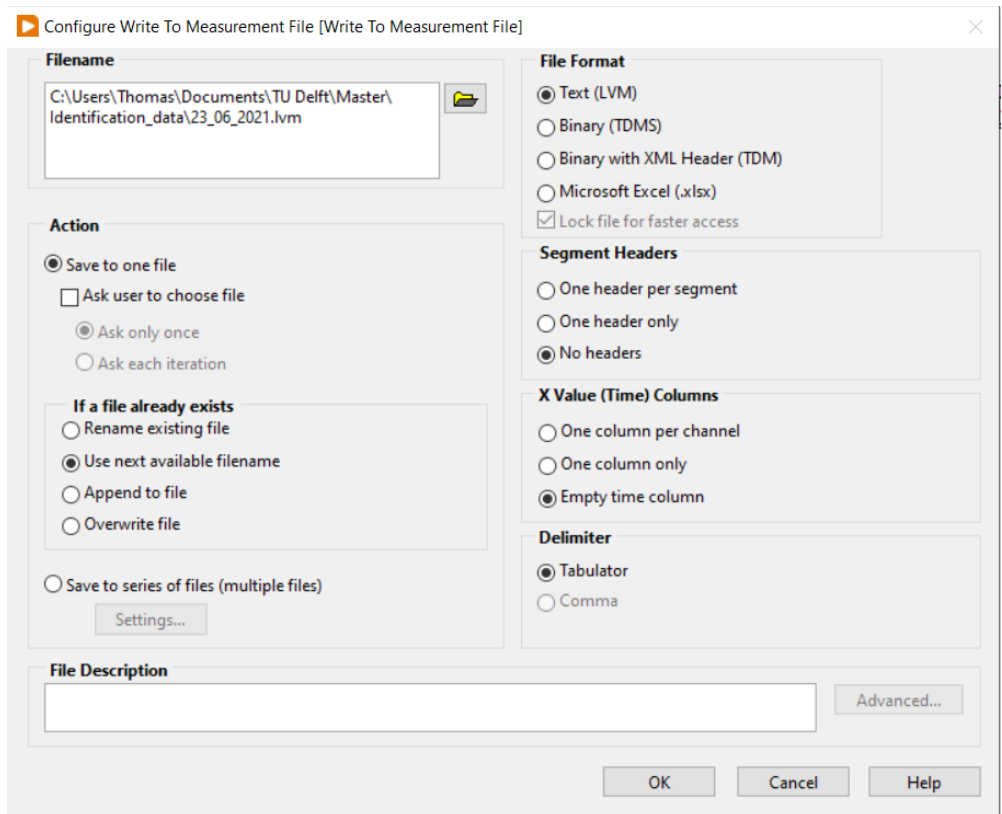


## From Measurement File to transfer function in Matlab – Step by step description

When a measurement is performed, a LVM file will be saved on the specified location. This LVM file could then be opened in Matlab Workspace. Typically, a data file of a measurement looks like this:

For data processing, it is the most easy to have column vectors that represent channels. So, in this case, there are 27 data channels, so 27 column vectors are needed. To make this easier, a function can be made in Matlab. This is done in the following way:
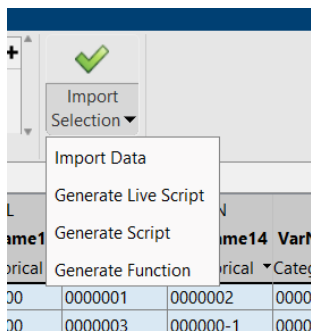
For Output Type, select Column vectors.
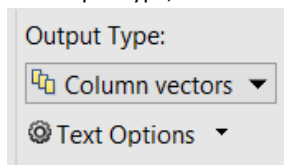
For Column delimiters, select comma.
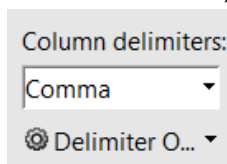
Click on the small arrow next to 'Import Selection' and select Generate function.

**B**

If 'Generate Function' is selected, Matlab will automatically make a function that imports the data file and generates column vectors for each of the channels of the data file. In the Matlab lines below, data from 4 different measurements stack actuation with no PPF, setup a, setup b and setup c are imported by using the function 'importfile7' that is automatically generated by Matlab by following the previous steps.

```
[A1, A2, A3, A4, A5, A6, A7, A8, A9, A10, A11, A12, A13, A14, A15,
A16, A17, A18, A19, A20, A21, A22, A23, A24, A25, A26, A27] =
importfile7('FRF_stack_noPPF.lvm'); %ACTUATION SIGNAL;

[a1, a2, a3, a4, a5, a6, a7, a8, a9, a10, a11, a12, a13, a14, a15,
a16, a17, a18, a19, a20, a21, a22, a23, a24, a25, a26, a27] =
importfile7('FRF_stack_PPFsetup_a.lvm'); %SETUP A;

[b1, b2, b3, b4, b5, b6, b7, b8, b9, b10, b11, b12, b13, b14, b15,
b16, b17, b18, b19, b20, b21, b22, b23, b24, b25, b26, b27] =
importfile7('FRF_stack_PPFsetup_b.lvm'); %SETUP B;

[c1, c2, c3, c4, c5, c6, c7, c8, c9, c10, c11, c12, c13, c14, c15,
c16, c17, c18, c19, c20, c21, c22, c23, c24, c25, c26, c27] =
importfile7('FRF_stack_PPFsetup_c.lvm'); %SETUP C;
```

For brevity, the next example will only focused on the 'no PPF' case. To find the transfer function of the other setups, the procedure is exactly the same.

First, the right channels are selected for the actuation signal, and all of the sensor signals. The first 1000 datapoints are omitted because this part of the data contains noise caused by switching on the measurement system, and the frequency sweep of the chirp signal has not started yet for these data points. In the following lines, it is shown how the channels are selected for the actuator and sensor signals.

```
%% Select the channels of disturbance actuator, sensors 1-7 and
accelerometer for all setups

U1 = A11(1000:end);%disturbance actuator
Y1 = A20(1000:end) %sensor 1
Y2 = A21(1000:end) %sensor 2
Y3 = A22(1000:end) %sensor 3
Y4 = A23(1000:end) %sensor 4
Y5 = A23(1000:end) %sensor 5
Y6 = A25(1000:end) %sensor 6
Y7 = A27(1000:end) %sensor 7
Y8 = A2(1000:end); %accelerometer
```

Then, the settings for the TF estimate function will be specified. Here, nfs is the number of entries that will be in the final tf estimated plot. Fs is the sampling frequency, and a Hanning window is used

```
%% TF estimate settings
nfs = 1.5e5; N = nfs*2/3; Fs = 1/100e-6; %tfestimate parameters, Fs
= 10 kHz
wind = hann(N+1); %Hanning window is used in tfestimate
```

Now, all settings for the tfestimate function are specified. The function can be computed, and also the coherence can be computed using the same settings. The lines below show how the transfer function of sensor 1 is calculated. The example shown here is for the accelerometer, but for the other sensors the procedure is exactly the same.

```matlab
% frequency response accelerometer
[TXY8,FT8] = tfestimate(U1,Y8,wind,[],nfs,Fs); %Estimate transfer
function for no PPF system
COHERENCE8 = mscohere(U1,Y8,wind,[],nfs,Fs);    %Coherence for no PPF
system
```

Finally, the estimated transfer function can be plotted. To compare the transfer functions of multiple setups (to evaluate the damping performance), the transfer functions of the different setups are plotted in the same figure. This is shown in the following part of the Matlab code, where the transfer function from the stack actuator to the accelerometer is computed for different setups.

```matlab
%% Plot Transfer function from disturbance actuator to accelerometer
figure(); sgtitle('Transfer Function Accelerometer'); hold on;
legend
subplot(3,1,1); semilogx(FT8,20*log10(abs(TXY8)),'k','DisplayName',
'no PPF'); title('Magnitude'); xlabel('f (Hz)'); ylabel('Gain
(dB)'); xlim([8 900]);grid;  hold on; grid;
subplot(3,1,2); semilogx(FT8,(180/pi*angle(TXY8)),'k');
title('Phase'); xlabel('f (Hz)'); ylabel('degree'); grid; xlim([8
900]);hold on; grid;
subplot(3,1,3); semilogx(FT8,COHERENCE8,'k'); title('Coherence');
xlabel('f (Hz)'); ylabel('Coherence'); grid; ylim([0 1.1]); xlim([8
900]); hold on; grid;

subplot(3,1,1); semilogx(ft8,20*log10(abs(txy8)),'b','DisplayName',
'PPF - Setup a'); title('Magnitude'); xlabel('f (Hz)'); ylabel('Gain
(dB)'); xlim([8 900]);grid;  hold on; grid;
subplot(3,1,2); semilogx(ft8,(180/pi*angle(txy8)),'b');
title('Phase'); xlabel('f (Hz)'); ylabel('degree'); grid; xlim([8
900]);hold on; grid;
subplot(3,1,3); semilogx(ft8,coherence8,'b'); title('Coherence');
xlabel('f (Hz)'); ylabel('Coherence'); grid; ylim([0 1.1]); xlim([8
900]); hold on; grid;

subplot(3,1,1);
semilogx(ft8b,20*log10(abs(txy8b)),'r','DisplayName', 'PPF - Setup
b'); title('Magnitude'); xlabel('f (Hz)'); ylabel('Gain (dB)');
xlim([8 900]);grid; legend; hold on; grid;
subplot(3,1,2); semilogx(ft8b,(180/pi*angle(txy8b)),'r');
title('Phase'); xlabel('f (Hz)'); ylabel('degree'); grid; xlim([8
900]);hold on; grid;
subplot(3,1,3); semilogx(ft8b,((coherence8b)),'r');
title('Coherence'); xlabel('f (Hz)'); ylabel('Coherence'); grid;
ylim([0 1.1]); xlim([8 900]); hold on; grid;

subplot(3,1,1); semilogx(ft8c,20*log10(abs(txy8c)),'Color',[0, 0.8,
0],'DisplayName', 'PPF - Setup c'); title('Magnitude'); xlabel('f
(Hz)'); ylabel('Gain (dB)'); xlim([8 900]);grid; legend('Location',
'northwest'); hold on
```
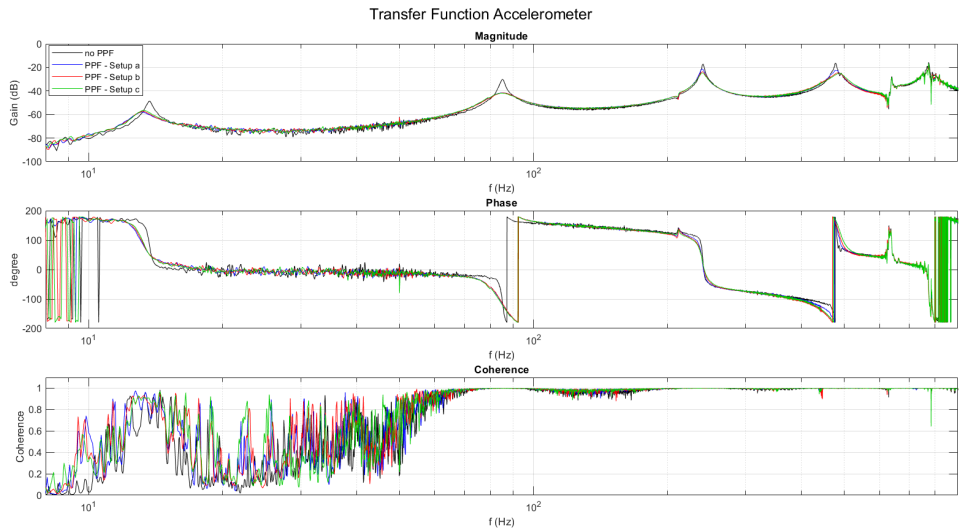
```
subplot(3,1,2); semilogx(ft8c,(180/pi*angle(txy8c)),'Color',[0, 0.8,
0]); title('Phase'); xlabel('f (Hz)'); ylabel('degree'); grid;
xlim([8 900]);hold on
subplot(3,1,3); semilogx(ft8c,coherence8c,'Color',[0, 0.8, 0]);
title('Coherence'); xlabel('f (Hz)'); ylabel('Coherence'); grid;
ylim([0 1.1]); xlim([8 900]); hold on
```

**B**

If this part of the code is runned in Matlab, the following plot is obtained.



In this plot, the transfer function from the stack to the accelerometer is shown for all of the 4 setups (no PPF, setup a, setup b and setup c). By zooming in on the resonance peaks, the damping performance can be analysed.

# C

# SYSTEM IDENTIFICATION

In this section, the system identification is shown. The system identification is performed by actuating one of the actuators with a chirp signal (sinusoid with increasing frequency). Then, the sensor signals are obtained, and a transfer function could be plotted (see appendix B for a detailed description of this process). On the next pages, the results of the system identification are shown.

## System identification

After assembling the setup, the system is identified. This is done by introducing a sinusoidal voltage in one of the actuators. This sinusoid has an increasing frequency. When the frequency sweep is performed, the sensor data is collected and processed in Matlab. Then, transfer functions from the disturbance actuation to the sensors could be computed. From these transfer functions, the resonance frequencies of the different vibration modes of the system can be obtained. Another aspect that could be useful is to test if the mode of interest is actually actuated by the intended actuators in a real-life setup.

First, the identification is performed on setup a (shown in the figure below). The four collocated transfer function will be shown.
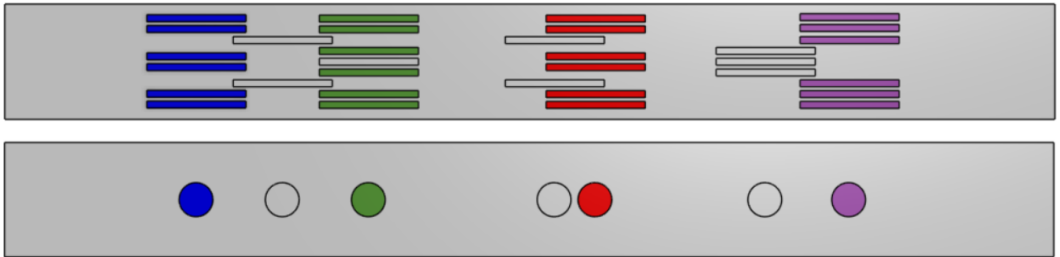


### Actuator 1 – Sensor 1 (mode 1). Collocated Transfer function
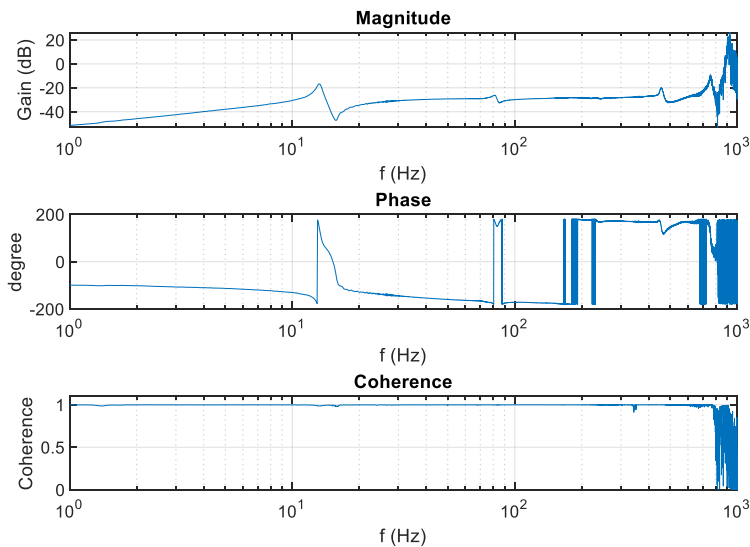


As expected, mode 1 is the highest peak in the magnitude plot. It can also be observed that the coherence is very good over the whole frequency range. This is expected for a collocated sensor-actuator pair.

## Actuator 3 – Sensor 3 (mode 3). Collocated Transfer function
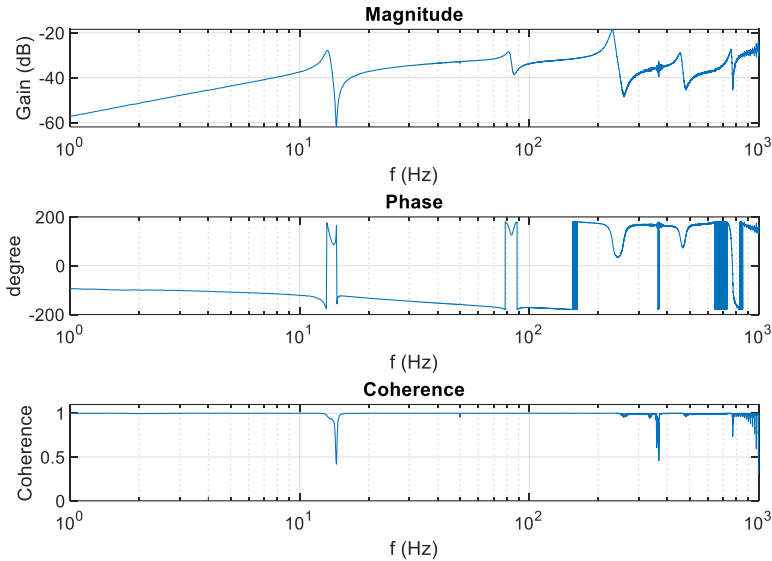
From this plot, it can be seen that the third mode (around 240 Hz) is the highest peak in the transfer function. Again, the coherence shows nicely collocated characteristics.

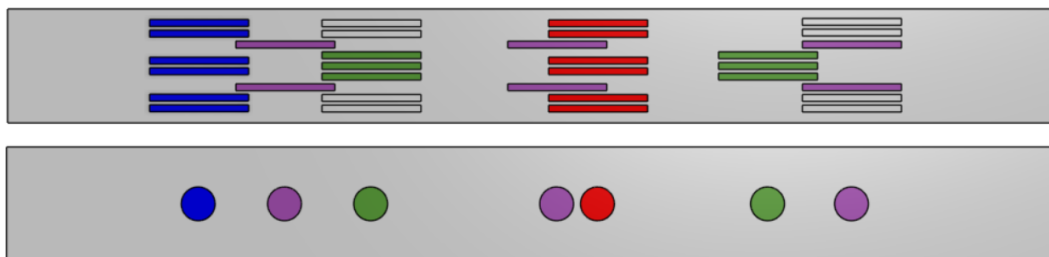## Actuator 5 – Sensor 5 (mode 2). Collocated Transfer function
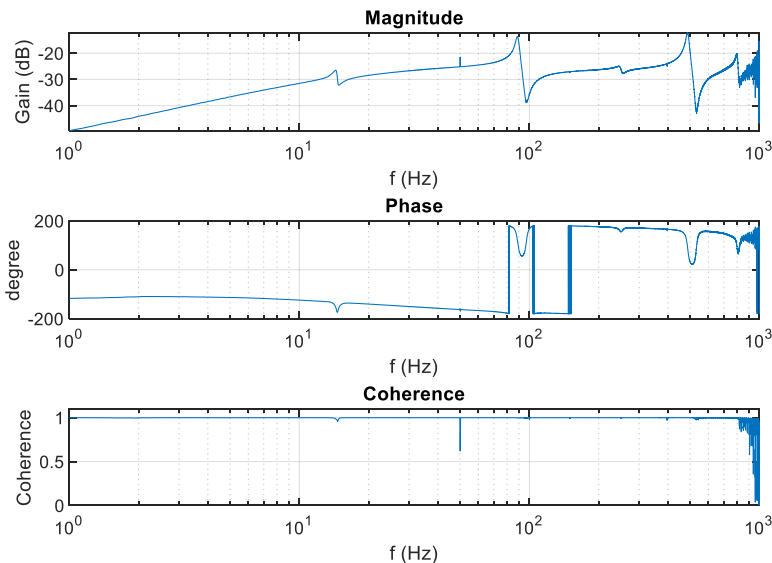


As expected, this plot shows mode 2 (and mode 4) as the highest peak in the magnitude plot. This is because the collocated sensor/actuator pair is located at the maximum modal strain location of mode 2. This is also very close to a maximal modal strain location for mode 4. Also, it can be observed that mode 3 is almost not excited by this actuator. This is because the actuator is located very close to a strain node of mode 3.
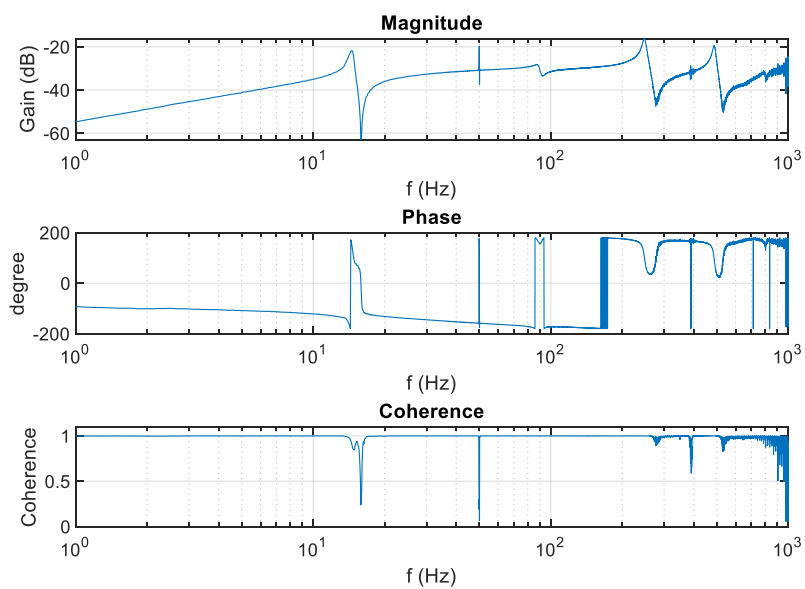
## Actuator 7 – Sensor 7 (mode 4). Collocated Transfer function
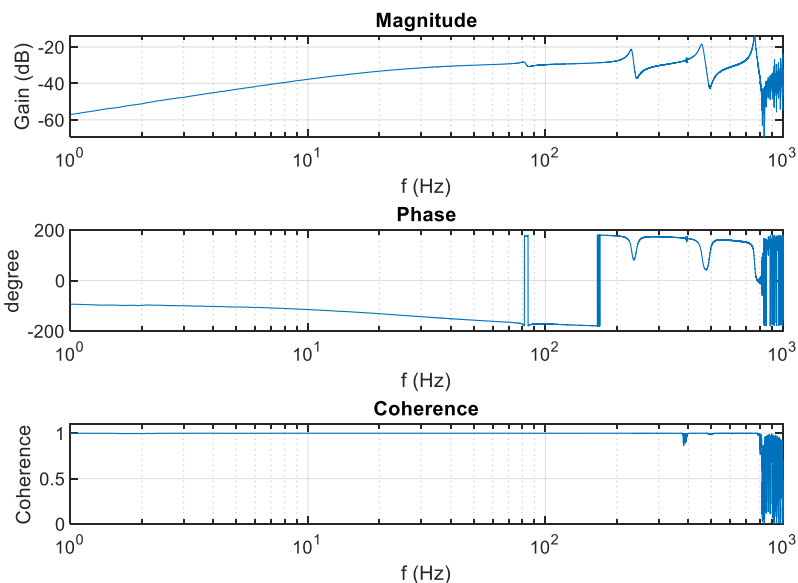


Again, this plot shows a nicely collocated behaviour. What can be observed from this transfer function is that the lower modes (mode 1 and 2) are almost not actuated by this actuator (and not observed by the collocated sensor). This is because the actuator is close to the tip of the beam, and the modal strain for mode 1 and 2 is low. Therefore, these modes are hardly excited and observed.

**System identification setup c (over-actuation and over-sensing)**



C

## Actuator 3 – Sensor 3 (mode 3). Collocated Transfer function

## Actuator 6 – Sensor 6 (mode 3). Collocated Transfer function
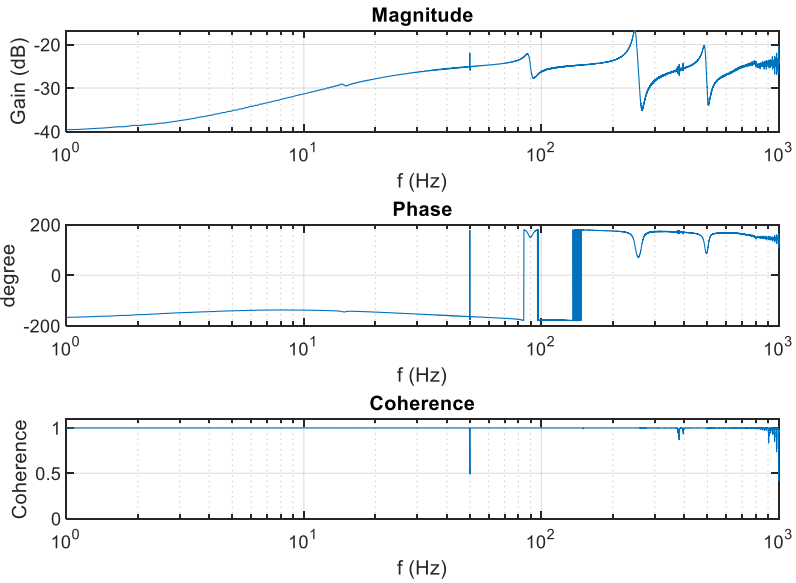


## Actuator 2 – Sensor 2 (mode 4). Collocated Transfer function
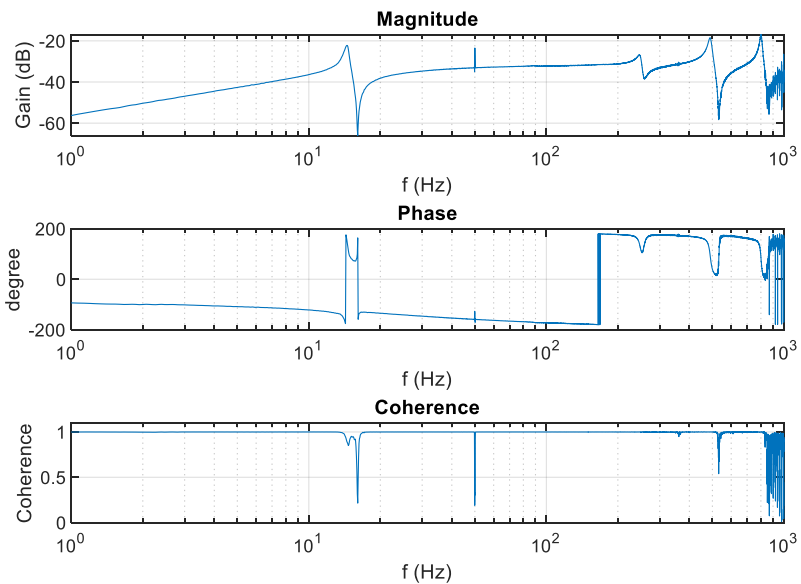
## Actuator 4 – Sensor 4 (mode 4). Collocated Transfer function
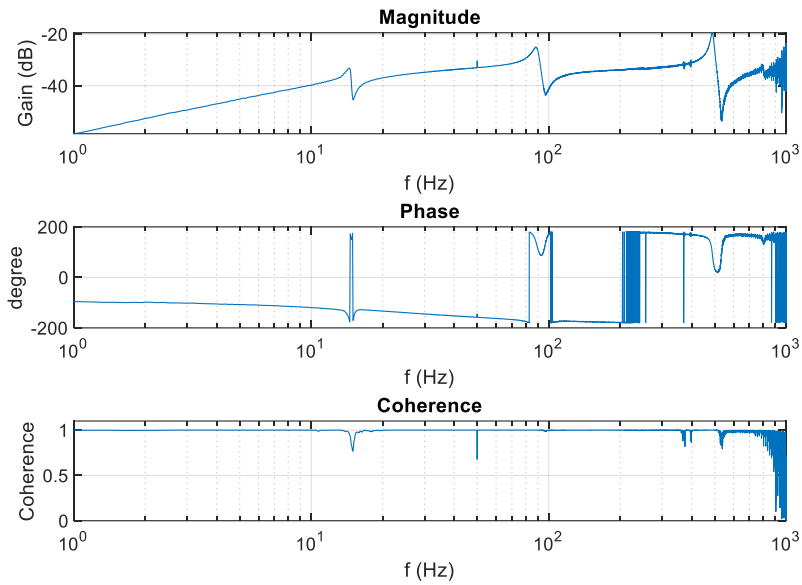
## Actuator 7 – Sensor 7 (mode 4). Collocated Transfer function
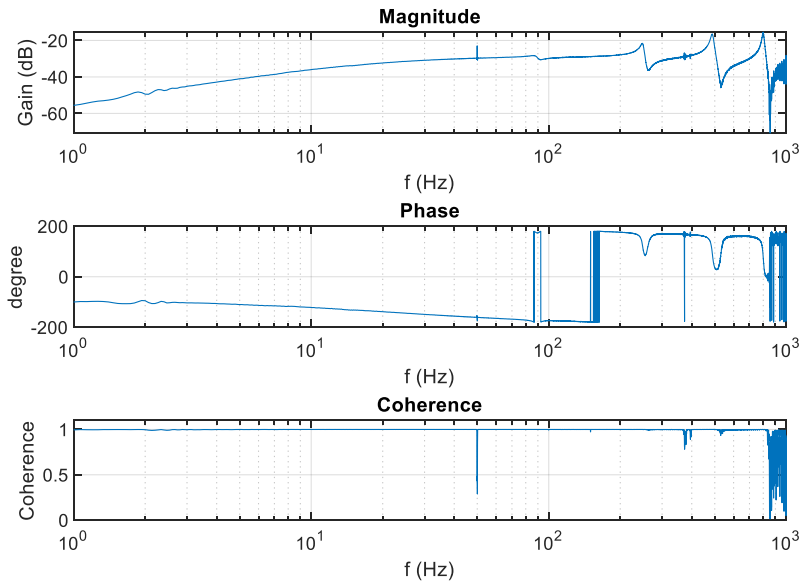
# D

## PRACTICAL WORK

In this appendix section, the practical work to create the experimental setup is explained. This section serves as a guide if someone wat to recreate the setups, or is interested in general tips in the gluing/handling of piezoelectric sensors and actuators.
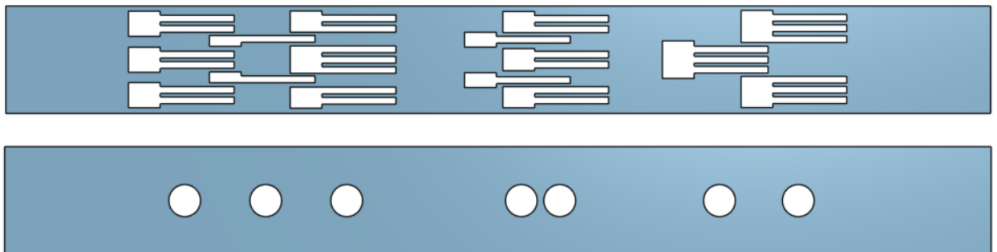
# Attaching sensors and actuators to the flexure

The flexure in the experimental setup is an aluminum strip (dimensions 370x40x2 mm). The piezoelectric sensors and actuators are attached to this setup using an epoxy. After testing multiple types of epoxy, it has been concluded that 'UHU Plus Endfest 300' (see picture below) is easy to use and fits the requirements. This is a 2 component Epoxy. The two components are mixed in a 1:1 ratio. After mixing, it can be processed for approximately 90 minutes before hardening. Then, it takes 12 hours to fully harden. After these 12 hours, the connection should be able to withstand forces of approximately 3 kN (300 kg).



For placing the sensors and actuators at the right location, a mold is 3d printed. This mold is made of PLA material, and the thickness is 1 mm. This is thick enough to securely place the sensors and actuators in the mold, but also thin enough so that it can be easily pealed off after gluing.

The molds for the sensors and actuators are shown below. For the actuators, a wider part is designed at the end of the holes to make sure that the can easily place the small actuators. For the sensor mold, the diameter of the circles is designed to be 0.1mm larger than the diameter of the sensor elements so that there will be no problems while trying to fit the sensors in the mold

For attaching the sensors and actuators to the flexure, the following procedure is used.

1. Use fine grid sandpaper to sand the surface of the aluminum flexure (to smoothen the surface and remove other residues)
2. Clean the surface of the flexure with aceton to remove any oils and grease
3. Put the mold on top of the flexure and connect it firmly using removable tape
4. Mix the two components of the 'UHU Plus' epoxy in a 1:1 ratio
5. Apply a thin layer of the mixed substance at the bottom surface of the actuator (or sensor) in an X-shape
6. Place the actuator (or sensor) in the mold at the desired location, and press on top of the actuator from the middle to the sides. This is done to make sure the epoxy glue in the X-shape is evenly distributed over the surface of the actuator
7. Repeat step 5 and 6 until all of the actuators (or sensors) are placed at the desired location
8. Put a few sheets of a4 paper on top of the whole beam (this is done to try to distribute the pressure from the added weight in step 9 in the most evenly distributed way)
9. Place a heavy flat object on top of this a4 paper. For example, a few textbooks can be used for this.
10. Make sure the heavy objects are on top of the whole beam for at least 12 hours
11. After at least 12 hours, the weights can be removed
12. Then, the molds can be removed (Be gentle! Don't use too much force). So, first the tape can be removed and then you should be able to gently remove the 3d printed mold
13. Inspect the glue layers. If all the previous steps are performed in the right way, the actuators (or sensors) should now be firmly attached to the beam!

The figures below show the gluing process. In the left figure, the mold (black color) is attached to the beam with tape (yellow color). The actuators are placed in the intended location and weights are placed on this setup for at least 12 hours. After removal of the weights and mold, the remaining setup is showed on the right. Here, all of the actuators are in the right place and are firmly attached to the flexure.
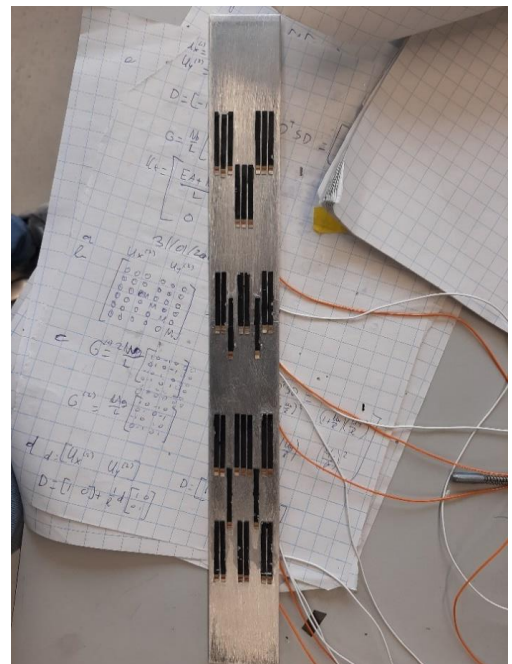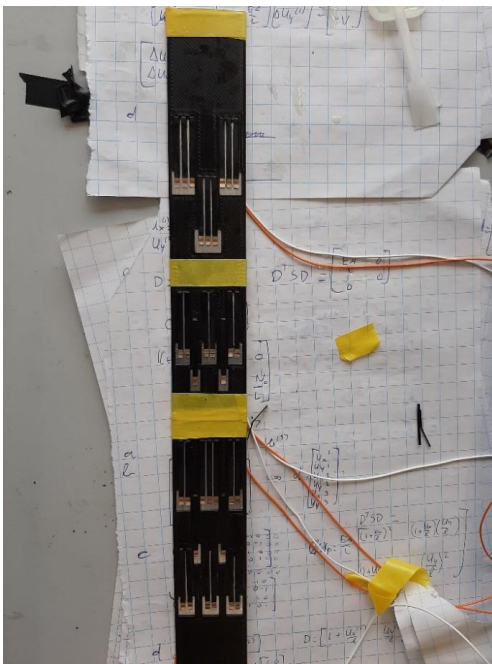
# Soldering wires to sensors and actuators

To connect the actuators and sensors to the amplifiers and CompactRIO, electrical wires are needed. After trying different types of wires, I have experienced that enamelled wire is the best option. The benefit from this type of wires is that it is very light, so the weight of the wires will not influence the system very much. Also, enamelled wire is relatively easy to solder to the small sensors and actuators. The downside of enamelled wire is that the coating is clear, and the wire is available in only 1 color. Therefore, it is hard to see which wire goes to which sensor/actuator. This is solved by using a color coding system, which is explained in the Appendix part on the experimental setup.

The wire that is used is a generic enamelled copper wire with a diameter of 0.20mm. The wire is insulated by a clear coating.

The soldering process is as follows:

1.  Cut the wire to the desired size (I used a length of approximately 120 cm to allow for some slack in the wires).
2.  Heat a soldering iron to around 350 degrees Celsius.
3.  Put the hot soldering iron at the end of the wire and add tin. In this way, the enamel coating will melt and a nice silver-like end part can be seen at the wire.
4.  Repeat step 3 for the other end of the wire.
5.  With both ends of the wire prepared, position the wire on the right connection pad of the actuator (or sensor).
6.  Heat the soldering iron to 300 degrees Celsius and press gently for a short time (1 second) on the wire and connection pad. If you are doing it correctly, the wire should now be nicely connected to the connection pod.
7.  Repeat these steps for all of the wires that need to be connected.
    **Pay attention!** Don't heat the piezoelectric actuator or sensor for to long (not longer than 1 second). This could cause the piezoelectric material to depolarize and therefore, performance will be decreased or even lost.